

Global aerosol climatology from the MODIS satellite sensors

Lorraine A. Remer,¹ Richard G. Kleidman,^{1,2} Robert C. Levy,^{1,2} Yoram J. Kaufman,^{1,3} Didier Tanré,⁴ Shana Mattoo,^{1,2} J. Vanderlei Martins,^{1,5} Charles Ichoku,^{1,6} Ilan Koren,⁷ Hongbin Yu,^{1,8} and Brent N. Holben⁹

Received 30 November 2007; revised 2 June 2008; accepted 9 June 2008; published 29 July 2008.

[1] The recently released Collection 5 Moderate Resolution Imaging Spectroradiometer (MODIS) aerosol products provide a consistent record of the Earth's aerosol system. Comparing with ground-based AERONET observations of aerosol optical depth (AOD) we find that Collection 5 MODIS aerosol products estimate AOD to within expected accuracy more than 60% of the time over ocean and more than 72% of the time over land. This is similar to previous results for ocean and better than the previous results for land. However, the new collection introduces a 0.015 offset between the Terra and Aqua global mean AOD over ocean, where none existed previously. Aqua conforms to previous values and expectations while Terra is higher than what had been expected. The cause of the offset is unknown, but changes to calibration are a possible explanation. Even though Terra's higher ocean AOD is unexpected and unexplained, we present climatological analyses of data from both sensors. We find that the multiannual global mean AOD at 550 nm over oceans is 0.13 for Aqua and 0.14 for Terra, and over land it is 0.19 in both Aqua and Terra. AOD in situations with 80% cloud fraction are twice the global mean values, although such situations occur only 2% of the time over ocean and less than 1% of the time over land. Aerosol particle size associated with these very cloudy situations does not show a drastic change over ocean, but does over land. Regionally, aerosol amounts vary from polluted areas such as east Asia and India, to the cleanest regions such as Australia and the northern continents. As AOD increases over maritime background conditions, fine mode aerosol dominates over dust over all oceans, except over the tropical Atlantic downwind of the Sahara and during some months over the Arabian Sea.

Citation: Remer, L. A., et al. (2008), Global aerosol climatology from the MODIS satellite sensors, *J. Geophys. Res.*, 113, D14S07, doi:10.1029/2007JD009661.

1. Introduction

[2] The instruments aboard NASA's Terra and Aqua satellites have been observing the Earth since early 2000 and mid-2002, respectively. In the words of Dr. Yoram J. Kaufman, Terra Project Scientist at the time of the Terra launch, the Terra and Aqua missions were "designed for a comprehensive check-up of planet Earth" (Y. J. Kaufman,

<http://terra.nasa.gov/Events/FirstImages/>, 2000). Similar to a checkup at the doctor's office, these missions would characterize the health of the planet. The goal was to use the vantage point of space to view the Earth's interconnected systems of atmosphere, land and ocean, and to characterize the parameters important to the sustainability of the planet and its human population.

[3] One important feature measured by several instruments aboard Terra and Aqua is atmospheric aerosol. These small solid or liquid particles suspended in the atmosphere play a major role in the energy balance of the Earth, in modifying cloud, precipitation, and atmospheric circulation characteristics, in providing nutrients to nutrient-limited regions of land and oceans, and in affecting air quality and public health. Aerosols are highly inhomogeneous in space, time and composition, and yet, knowing the amount, composition, distribution, size and shape of these particles is necessary for any meaningful estimates of their effect, from estimating anthropogenic climate forcing to forecasting air quality and potential health effects from air pollution.

[4] One of the instruments aboard both Terra and Aqua used to characterize atmospheric aerosols is the Moderate

¹Laboratory for Atmospheres, NASA Goddard Space Flight Center, Greenbelt, Maryland, USA.

²Science Systems and Applications, Inc., Lanham, Maryland, USA.

³Deceased 31 May 2006.

⁴Laboratoire d'Optique Atmosphérique, Villeneuve d'Ascq, France.

⁵Department of Physics, University of Maryland, Baltimore County, Baltimore, Maryland, USA.

⁶Earth System Science Interdisciplinary Center, University of Maryland, College Park, Maryland, USA.

⁷Weizmann Institute, Rehovot, Israel.

⁸Goddard Earth Science and Technology Institute, University of Maryland, Baltimore County, Baltimore, Maryland, USA.

⁹Laboratory for Terrestrial Physics, NASA Goddard Space Flight Center, Greenbelt, Maryland, USA.

Resolution Imaging Spectroradiometer (MODIS). The aerosol product derived from MODIS observations now includes a 7 year record from Terra-MODIS and a 5 year record from Aqua-MODIS. We are now at a point to use this information in the manner intended, to perform a quantitative “checkup” of Earth’s global aerosol system. How are aerosols distributed over the continents and oceans? How are different sizes distributed, and what are the relationships between aerosol loading and aerosol particle size in different regimes? Finally, what are the regional and seasonal characteristics of the aerosols? In this paper we will attempt to answer these questions from the database of MODIS aerosol products.

[5] MODIS is not the only satellite instrument used to characterize atmospheric aerosols, nor is it the first. In fact, the first attempts at creating an aerosol climatology from observations did not use satellite instruments at all. In situ measurements on the ground and from aircraft, and ground-based remote sensing observations provided initial characterization of the distribution of aerosol types and loading [d’Almeida *et al.*, 1991; Holben *et al.*, 2001, and references therein]. Further compilations extended the primarily land-based climatology to oceans via shipboard observations [Smirnov *et al.*, 2002, and references therein], and advances in ground-based remote sensing and inversion methods permitted more detailed characterization of aerosol properties [Dubovik *et al.*, 2002]. However, satellite retrievals gave us our first global view of the aerosol system. Beginning with the Advanced Very High Resolution Radiometer (AVHRR) retrievals of aerosol optical depth in one wavelength over oceans [Husar *et al.*, 1997] we began to see regional and seasonal distributions of major aerosol systems. The AVHRR picture expanded to include quantitative particle size information [Geogdzhayev *et al.*, 2002, 2005], but continued to be limited to oceans. Another early sensor, the Total Ozone Mapping Satellite (TOMS) provided its own global, regional and seasonal portrayal of the aerosol system over land and ocean [Torres *et al.*, 2002], but was limited to aerosol optical depth in the ultraviolet spectral region.

[6] Modern satellite sensors including Polarization and Directionality of the Earth’s Reflectances (POLDER), Multiangle Imaging Spectroradiometer (MISR), Ozone Monitoring Instrument (OMI) and MODIS now have sufficiently long data records to produce their own global, regional and seasonal climatologies [Liu *et al.*, 2006; Yu *et al.*, 2006]. All these data sets produce a *qualitatively* similar view of the Earth’s aerosol system. However, *quantitative* analysis reveals significant differences in mean aerosol optical depth and other aerosol parameters retrieved from satellite [Mishchenko *et al.*, 2007]. Resolving quantitative differences between satellite-derived aerosol products is an ongoing challenge for the research community. One step in meeting this challenge is to provide quantitative analyses of the statistical results of each individual sensor’s data record, thereby providing a basis for comparison and evaluation.

[7] The paper first discusses the MODIS aerosol retrieval and evaluates the recent results derived from the Collection 5 algorithm against ground-based observations. Then, the Collection 5 results are compared with Collection 4 results to show the differences between the Collections and between Terra and Aqua. Once the Collection 5 results are put

into context, they are used to portray the global, regional and seasonal distribution of aerosol optical depth and particle size information.

2. MODIS Aerosol Products

[8] The aerosol products are derived operationally from spectral radiances measured by MODIS. MODIS has 36 channels spanning the spectral range from 410 to 14400 nm representing three spatial resolutions: 250 m (2 channels), 500 m (5 channels), and 1 km (29 channels). The aerosol retrieval makes use of seven of these channels (470–2130 nm) to retrieve aerosol characteristics [Remer *et al.*, 2005] and uses additional wavelengths in other parts of the spectrum to identify and mask out clouds and suspended river sediments [Ackerman *et al.*, 1998; Gao *et al.*, 2002; Martins *et al.*, 2002; Li *et al.*, 2003]. The MODIS aerosol algorithm is actually three independent algorithms, two derive aerosol characteristics over land and the other over ocean. The original land algorithm is based on the “dark target” approach [Kaufman and Sendra, 1988; Kaufman *et al.*, 1997; Remer *et al.*, 2005] and therefore does not retrieve over bright surfaces including snow, ice and deserts. A more recent MODIS product, labeled “Deep Blue” does retrieve over bright surfaces [Hsu *et al.*, 2004]. However, the climatology presented in this paper does not include the “Deep Blue” results. The ocean algorithm masks out suspended river sediments, clouds and sun glint, then inverts the radiance at 6 wavelengths (550 to 2130 nm) to retrieve aerosol optical depth (AOD) and particle size information [Tanré *et al.*, 1996, 1997].

[9] We will examine two types of aerosol products: aerosol optical depth (AOD) and particle size parameter. AOD (also referred to as aerosol optical thickness, AOT) is a straightforward measure of column integrated extinction. The MODIS product includes retrievals of AOD at seven wavelengths over ocean (470 nm, 550 nm, 660 nm, 870 nm, 1240 nm, 1630 nm and 2130 nm) and three wavelengths over land (470 nm, 550 nm, and 660 nm). There are several measures of particle size included in the MODIS aerosol product. Angstrom exponent over land is defined as:

$$AngExp = - \frac{\ln(AOD_{470}/AOD_{660})}{\ln(470/660)} \quad (1)$$

There are two Angstrom exponents over ocean, defined as

$$AngExp1 = - \frac{\ln(AOD_{550}/AOD_{870})}{\ln(550/870)} \quad (2)$$

and

$$AngExp2 = - \frac{\ln(AOD_{870}/AOD_{2130})}{\ln(870/2130)} \quad (3)$$

where AOD470, AOD550, AOD660, AOD870 and AOD2130 are the aerosol optical depths at the wavelengths specified, 470, 550, 660, 870 and 2130 nm, respectively. Angstrom exponent is a measure of the spectral dependence of the aerosol optical depth and a proxy for aerosol size. Larger Angstrom exponents indicate the dominance of

smaller particles, and vice versa. The MODIS aerosol product defines the Angstrom exponent over land with the 470 nm and 660 nm wavelengths because these represent the spectral range of the AOD retrieval over land, which is limited to only three wavelengths in the visible. The MODIS-retrieved spectral range of AOD over ocean spans seven wavelengths from the visible into the short-wave infrared. The product includes two ocean Angstrom exponents across this range in order to detect spectral curvature, and aid in identifying particle sizes and types [Eck et al., 1999].

[10] There are two other measures of particle size in the MODIS aerosol product, and these are fine aerosol optical depth (fine AOD) and fine mode fraction (FMF). Fine AOD is the aerosol optical depth attributed to submicron particles. These particles are sometimes described as accumulation mode particles and generally originate from combustion processes. Fine mode fraction is the ratio of fine AOD to total AOD, and describes the fraction of the AOD contributed by fine mode sized particles. There are subtle differences in exactly how fine AOD and FMF are defined in the MODIS algorithm over land and ocean [Levy et al., 2007a; Remer et al., 2006], and these definitions may differ from how other data systems define the same or similar parameters [O'Neill et al., 2003; Kleidman et al., 2005]. However, those details are well documented in the above cited literature and will not be reiterated here.

[11] The derived aerosol products undergo rigorous testing and validation. The algorithms were created before Terra launch and tested using data from airborne imagers [Kaufman et al., 1997; Tanré et al., 1997, 1999; Chu et al., 1998]. The results of these field tests coupled with sensitivity studies [Kaufman et al., 1997; Tanré et al., 1997] suggested that 1 standard deviation (1σ) of retrievals would fall within $\pm (0.03 + 0.05 \tau)$ over ocean and $\pm (0.05 + 0.15 \tau)$ over land, where τ is AOD. These error bounds, derived prelaunch are referred to as the “expected error.”

[12] After Terra launch, the products were validated by comparison with collocated ground-based observations by the Aerosol Robotics Network (AERONET). The AERONET network consists of hundreds of automatic instruments that measure aerosol optical depth (AOD) to within 0.01 accuracy [Holben et al., 1998; Eck et al., 1999; Smirnov et al., 2000], and retrieve other aerosol characteristics including particle size information [Dubovik and King, 2000; O'Neill et al., 2003]. Comparison of MODIS-derived AOD with collocated AERONET-measured data evaluated the percentage of MODIS retrievals that fell within the expected error bounds defined above [Ichoku et al., 2002, 2005; Remer et al., 2002, 2005; Levy et al., 2003, 2005]. Depending on wavelength, the number of ocean AOD retrievals confined to expected error bounds ranged from 60% to 70%. Additional validation using the NASA Ames Airborne Tracking Sun photometer confirmed that more than 1σ of MODIS ocean AOD values were retrieved within expected error bounds [Russell et al., 2007; Livingston et al., 2003; Redemann et al., 2005, 2006]. Over land, the comparison yielded varying results. In some cases the over land AOD retrievals fell within expected uncertainties ($\pm 0.05 \pm 0.15 \tau$) [Chu et al., 2002; Ichoku et al., 2002; Remer et al., 2005], but in many situations there appeared to

be a strong positive bias at low AOT in the over land retrieval, and a negative bias at high AOT [Ichoku et al., 2003, 2005; Levy et al., 2005; Remer et al., 2005]. The MODIS particle size information over ocean correlated well with AERONET retrievals, but tended to over predict the occurrence of small particles at the expense of large particles [Kleidman et al., 2005].

[13] To address these lingering problems with the aerosol products, new codes were developed. The land algorithm underwent significant change, while maintaining the basic dark target approach [Levy et al., 2007a, 2007b]. The ocean algorithm remained almost the same with changes made only to the assumed characterization of the sea salt particles in the retrieval. These new algorithms were applied operationally to the complete record of calibrated radiances to generate a new “collection” of aerosol products. These reprocessed data are known as Collection 5, which are available for both the Terra and Aqua records. Collection 5 provides us with a consistent data set created from a single set of algorithms applied identically to an uninterrupted data stream of calibrated radiances.

3. Data for the Climatology

[14] Two types of MODIS data will be used in this paper: Level 2 (L2) and Level 3 (L3). MODIS L2 aerosol data are ungridded 10 km retrievals of various aerosol parameters available at the time of satellite overpass. These data represent the fundamental MODIS aerosol product. The product consists of geophysical parameters such as aerosol optical depth and aerosol particle size information, as well as a quality assurance (QA) flag that indicates the level of reliability of each retrieval. QA flags range from 0 (lowest quality) to 3 (highest quality). Comparison of the L2 data, collocated in time and location with high-quality ground measurements provide the “validation” of the basic product.

[15] MODIS L3 data are an aggregation of the L2 data onto a gridded $1^\circ \times 1^\circ$ global grid and represent the statistics including the mean and weighted means of the L2 product contained within the grid square. L3 data are available on a daily basis. The daily L3 data are further aggregated to create L3 monthly means, also on a $1^\circ \times 1^\circ$ global grid. The global gridded data of L3 will provide the basic set of data for the climatology presented here.

[16] Creating daily L3 from L2, and further processing the data to achieve global and regional monthly means requires decisions as to how to aggregate and average the data at each step. Depending on what processing is chosen, variations in the final values can vary by as much as 20%. In this work we start with high-quality daily L3 data, weight by the number of L2 retrievals in the 1° grid square and calculate monthly means and other statistics. The reason for this decision is to minimize the contribution of retrievals in cloud fields, where artificially enhanced AOD occurs frequently [Zhang et al., 2005; Wen et al., 2006, 2007; Koren et al., 2007]. We show explicitly in section 7 the differences in AOD retrievals in highly cloudy situations, and discuss the possible reasons for the enhancement. It is incongruous for the monthly mean of a particular grid square determined by just one 10 km retrieval on 1 day of the month to count equally with another grid square that consisted of hundreds of 10 km retrievals in that month. On the other hand, we

want global representation of the data without contributions from QA = 0 data. Note, weighting the quality weighted product in this manner is not the same as making the same calculations directly from the 10 km L2 data.

4. Comparison of Collection 5 Against AERONET Observations

[17] We evaluate the Collection 5 aerosol products by comparing with collocated AERONET observations. A preliminary evaluation was performed and reported by *Levy et al.* [2007b] and *Remer et al.* [2006], but that evaluation was confined to a test bed of MODIS radiance granules. We note that while the test bed produced a substantial number of collocations, it was still limited in time and space. Furthermore, the test bed consisted of saved Collection 4 radiances. When Collection 5 was processed, not only were the aerosol retrieval algorithms upgraded to Collection 5, but the basic calibration coefficients were changed as well. Thus, the radiances used to create Collection 5 aerosols are different than those used for Collection 4. When we compare MODIS aerosol products to AERONET now, we evaluate simultaneously both the changes we made to the aerosol algorithms and the changes made to the calibration that provides the input to the aerosol retrieval.

[18] Figure 1 shows the results of collocating MODIS aerosol optical depth retrievals with AERONET for the ocean retrieval following the spatiotemporal technique of *Ichoku et al.* [2002]. This technique subsets a grid of 5 by 5 aerosol retrievals, centered on an AERONET station. Each MODIS aerosol retrieval nominally represents a 10 km area, thus the subsetted area, centered on the AERONET station, includes an area of approximately 50 km by 50 km. The spatial statistics of the MODIS retrievals in the 5 by 5 subset are calculated and compared to the temporal statistics of the AERONET observations taken ± 30 min of MODIS overpass. At least 5 of the possible 25 MODIS retrievals, and 2 of the possible 4 or 5 AERONET observations are required in order to keep the collocation in the comparison database. Thus, the collocation may not include the exact 10 km MODIS aerosol retrieval in which the AERONET station resides, but instead include retrievals up to 20–25 km away from the station. This is especially important in terms of the ocean retrieval because there are no MODIS ocean aerosol retrievals directly over land-based AERONET stations. By comparing spatiotemporal statistics rather than exact matchups the method relies on the general homogeneity of the aerosol field over 50 km [*Anderson et al.*, 2003] and permits a much larger collocation database, including ocean retrievals. Using this technique, a coastal AERONET site can be used simultaneously as validation for both land and ocean MODIS aerosol retrievals.

[19] We use AERONET Version 2.0, Level 2 Quality Assured data for the collocations (http://aeronet.gsfc.nasa.gov/new_web/Documents/version2_table.pdf). The database consists of a total of 326 AERONET stations, some permanent and some ephemeral, with 205 used exclusively for land, 40 for ocean and 81 contributing to both land and ocean. The time period of collocations spans March 2000 through November 2007 for Terra, and July 2002 through November 2007 for Aqua. Altogether there are over 11,000 collocations meeting our criteria for Terra land, over 8,000

for Aqua land, approximately 8,000 and 6,500 for Terra and Aqua ocean at 550 nm, respectively, and somewhat more collocations for ocean at 870 nm. The reason for different numbers of collocations for the different wavelengths has to do with the variety of spectral configurations of the AERONET stations, some of which have a 500 nm channel, and some that do not. We interpolate the AERONET observed AOD to the MODIS channel, but avoid large spectral adjustments. Therefore, if the 500 nm channel is missing from the AERONET station we do not include it in the 550 nm validation.

[20] Two wavelengths and both Terra and Aqua are shown in Figure 1. The ocean comparison is made for any island or coastal AERONET station within 25 km of the ocean. The only station eliminated from this analysis is Mauna Loa because of its high elevation in comparison to the ocean surface. All data with quality greater than 0 are included in these plots. The plots show data that were sorted according to AERONET AOD, grouped into 25 bins of near equal samples whose mean and standard deviation were calculated. The linear regression equations plotted and correlation coefficients indicated were calculated from the full cloud of collocated points before binning and averaging. The data used in this plot spans the length of the mission from March 2000 through November 2007 for Terra, and July 2002 through November 2007 for Aqua.

[21] MODIS aerosol optical depth retrieved over ocean is strongly correlated to the corresponding AERONET values for both wavelengths and both satellites. Expected error for ocean retrievals is $\pm (0.03 + 0.05 \tau)$. AOD retrievals at the 870 nm channel fall within expected error more than 2/3 of the time. Retrieval results for shorter wavelengths are less consistently accurate, falling within expected error only 60% of the time at 550 nm. These results for Collection 5 are similar to those reported for Collection 4 [*Remer et al.*, 2005].

[22] Figure 2 shows the results of comparing Collection 5 retrievals over land with AERONET AOD. Again these are “global” plots making use of all AERONET stations except COVE and Venise, which are both located on stand alone ocean platforms far from shore. For land we use those retrievals with the highest-quality labels (QA = 3). Over land, the inclusion of lower-quality retrievals will make a significant difference in the validation plots, lowering the correlation and decreasing the percentage of retrievals within expected error. We recommend to users to check quality flags over land and to use retrievals with QA < 3 only qualitatively. For ocean, as long as QA > 0 we find the retrievals accurate and quantitatively useable [*Russell et al.*, 2007]. The land and ocean retrievals are different algorithms and the QA flags simply have different meanings in the two algorithms. Similar numbers of collocations are available for both land and ocean despite the fact that there are many more AERONET stations over land than near ocean. The requirement on the land quality flag eliminates many collocations from the analysis. Thus, while there are more opportunities to compare with AERONET over land, there are fewer locations where a high-quality land retrieval is possible. The plots in Figure 2 are prepared in the same manner as in Figure 1, although only the 550 nm channel is shown because there is no 870 nm retrieval over land.

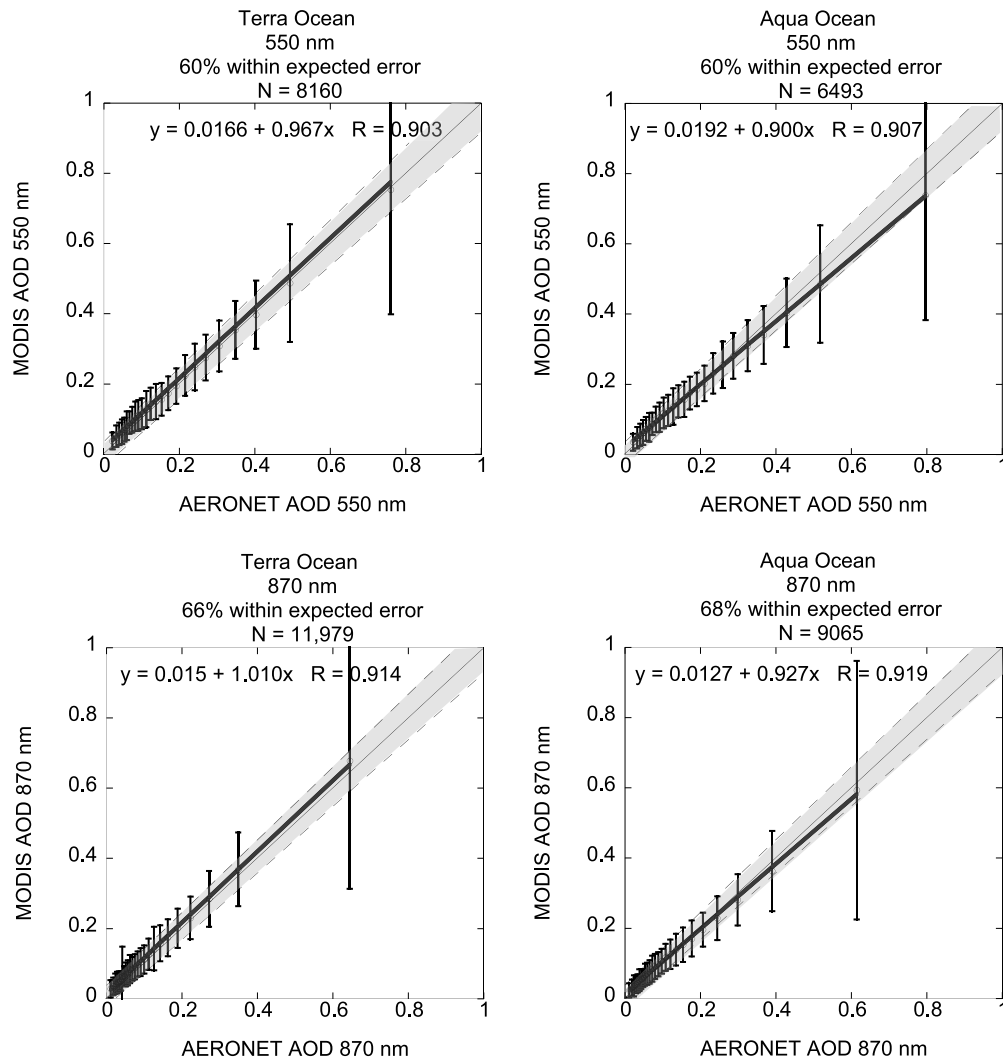


Figure 1. MODIS aerosol optical depth (AOD) over oceans plotted against collocated AERONET observations. (top) AOD at 550 nm. (bottom) AOD at 870 nm. (left) Collocations with the Terra satellite. (right) Collocations with the Aqua satellite. The data were sorted according to AERONET AOD and divided into 25 bins of equal observations, and statistics were calculated. Points represent the means of each bin. Error bars represent the standard deviation of MODIS AOD within those bins. Highest AOD bin typically represents the mean of fewer observations than the other bins. AERONET AOD at 550 nm was interpolated on a log-log plot between observations at 500 nm and 675 nm. Stations with no 500 nm channel were not included in Figure 1 (top) but were included in Figure 1 (bottom) where no interpolation was necessary. The regression line, regression equation, and correlation were calculated from the full cloud of points before binning. Expected error is $\pm(0.03 + 0.05 \cdot \text{AOD})$ and is shown in the plots by the dashed lines.

[23] MODIS aerosol optical depth over land in Collection 5 is an improvement of the results from Collection 4 [Remer *et al.*, 2005]. More than 72% of retrievals fall within expected error over land at 550 nm. In Collection 4, 68% of retrievals fell within expected error at that wavelength. More importantly there was a 41% overall positive mean bias in Collection 4, indicating that mean MODIS AOD is 41% higher than mean AERONET AOD in the collocation data set. In Collection 5 the bias is almost insignificant, with 0 mean bias in Terra and $\sim 7\%$ bias in Aqua. Note that the expected error over land $\pm (0.05 + 0.15 \tau)$ is greater than that over ocean $\pm (0.03 + 0.05 \tau)$.

[24] The comparison of AOD retrievals over land and ocean show that the Collection 5 retrieval is producing results either as accurate as Collection 4 (ocean) or much improved (land), at least in a global sense. There appears to be little difference between Terra and Aqua. Validation efforts beyond the scope of this paper continue. Individual regions will be examined, and we will include ship board measurements as well as AERONET observations as the “ground truth.” Another point not addressed in this paper is the validation of the size parameter products in Collection 5. However, for now, we see that the MODIS Collection 5

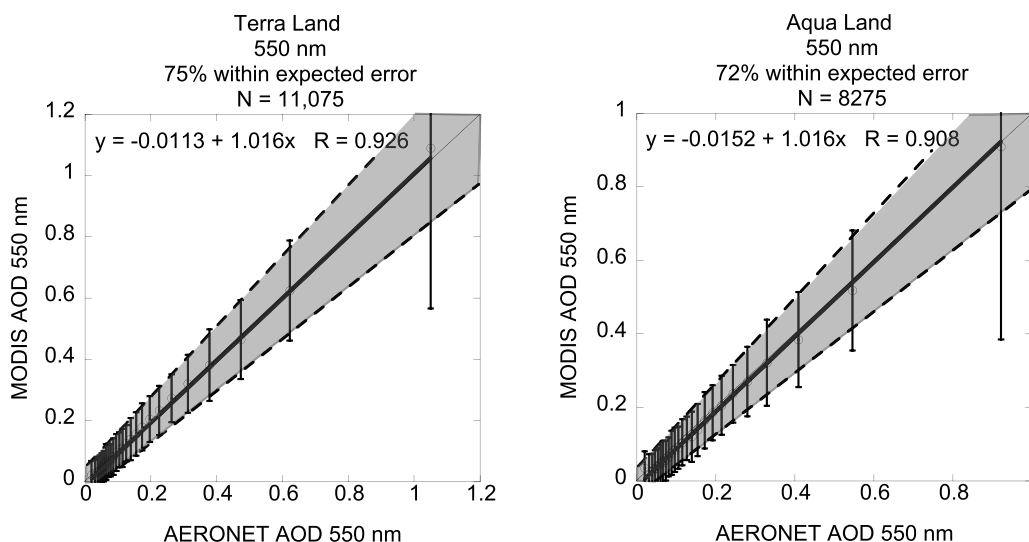


Figure 2. Similar to Figure 1 but for collocations over land. The land product does not include a retrieval at 870 nm. Expected error over land is $\pm(0.05 + 0.15 \cdot \text{AOD})$. Note that the scales for Terra and Aqua are different.

aerosol product can be used to examine the state of the aerosol system.

5. Comparison of Collection 5 With Collection 4

[25] By comparing MODIS retrieved AOD with collocated AERONET observations on a day by day basis we established that the Collection 5 retrievals are a fair representation of the Earth's aerosol system, to within specified accuracies. Even if both Collection 5 and Collection 4 [Remer *et al.*, 2005] aerosol optical depth match AERONET observations within MODIS specifications, there could still be systematic offsets. In this section we compare mean results of the two Collections.

[26] Over ocean, the only difference between Collection 4 and Collection 5 aerosol algorithms is that assumptions about the optical properties of sea salt particles were adjusted to better match more recent observations [Remer *et al.*, 2006]. AERONET retrievals of aerosol optical properties available only after Terra-MODIS launch suggested that the real part of the refractive index for sea salt particles was smaller than the 1.43 used in the original algorithm. The real part refractive index of sea salt particles in the ocean algorithm was changed to 1.35 in accordance with Dubovik *et al.* [2002] and O. Dubovik *et al.* (personal communication, 2007). The consequence of this change was tested by applying the altered algorithm to our test bed of saved Collection 4 radiances. The results are shown in Figure 3. The changes reduced the positive bias in the fine mode fraction retrieved by Collection 4 [Kleidman *et al.*, 2005], while not making any significant changes to the AOD retrieval. Both Aqua and Terra data were used during testing. The mean AOD using either software was 0.15, but the mean fine mode fraction changed from 0.47 to 0.39. Thus we did not expect any changes to the AOD from Collection 4 results, but did expect reduced fine mode fraction.

[27] Figure 4 shows a comparison of monthly global mean AOD over oceans between Collection 4 and Collec-

tion 5 for Terra-MODIS and Aqua-MODIS. Unlike Figure 3 the data used to create Figure 4 do not come from our saved test bed of radiances. These data, instead, come directly from the operational database available to all users. The Collection 4 AOD values were processed with Collection 4 radiances as input, while the Collection 5 AOD values were processed with Collection 5 radiances as input. Note that updates in calibration cause Collection 5 radiances to differ from Collection 4. The data plotted include only the period of overlap of all four data sets, from August 2002 when Aqua began processing data to August 2005 when Collection 4 production ended. In Figure 4 we see that for the

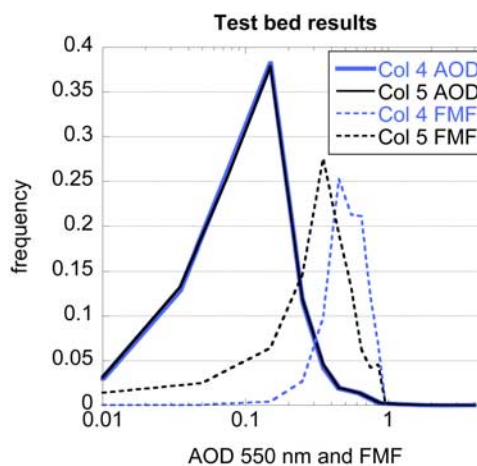


Figure 3. Histogram of aerosol optical depth at 550 nm (AOD) over ocean and fine mode fraction (FMF) derived from MODIS aerosol algorithms applied to a test bed of saved collection 4 radiances. The test bed consisted of 35 granules of various oceanic aerosol scenes spread throughout 2001. Over 400,000 retrievals were used to construct the histograms. The Collection 4 results are shown in blue. Results of applying Collection 5 software to Collection 4 radiances are shown in black. Solid curves denote AOD, and dotted curves denote FMF.

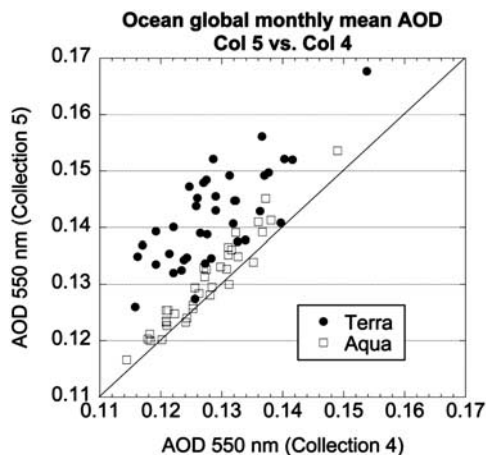


Figure 4. Global and monthly mean aerosol optical depth (AOD) at 550 nm over the global oceans from operational Collection 5 processing plotted against similar produced from old Collection 4 processing. Collection 5 processing includes both updates to the aerosol algorithm and also updates to the calibration. Terra and Aqua are plotted separately. Terra Collection 5 is higher than Terra Collection 4, and also higher than both Aquas.

Aqua satellite there is only a slight bias between Collections, as expected, but for Terra Collection 5 it is approximately 0.015 higher than Collection 4. Note that 0.015 is well within the expected error of $\pm (0.03 + 0.05 \tau)$. Further analysis shows that Terra Collection 4 matches both Aqua Collections and that Terra Collection 5 is an outlier when compared to the other three data sets.

[28] The 0.015 offset in ocean AOD between Terra Collection 5 and the other three data sets is not yet understood. Algorithm changes were applied equally to the software run for Terra and Aqua. If an AOD offset was introduced by the changes described above, then we would see AOD changes equally in both satellites. Because the offset has been introduced to Terra and not Aqua, we suspect this offset is due to updates to the Terra-MODIS calibration constants that altered the Collection 5 input radiances. We note that Terra's coefficients were adjusted up to 2% depending on wavelength, while adjustments to Aqua's coefficients were less than 0.5% (MODIS Characterization Science Team, personal communication, 2007). The differences between Collection 4 and Collection 5 and between Terra and Aqua retrievals that now exist over ocean illustrate some of the limitations and uncertainties of the product. While these uncertainties should be noted they do not invalidate the agreement seen in comparison to AERONET observations, nor the ability of the MODIS aerosol product to describe the global, regional and seasonal patterns of the ocean aerosol system, to within the stated uncertainties.

[29] Over land, in contrast to ocean, substantial differences exist between the Collection 4 and 5 algorithms [Levy *et al.*, 2007a, 2007b]. All assumptions about aerosol optical properties were modified, as were surface assumptions and snow masking. Small negative AOD retrievals were permitted in recognition that the MODIS land aerosol algorithm is insensitive to AOD less than 0.05 and that

arbitrarily excluding negative retrievals artificially introduces a positive bias in nearly clean conditions. A vector radiative transfer code replaced the scalar code used in Collection 4, and the overall inversion scheme was changed. Because of these changes we expect Collection 5 to have substantially different AOD values than Collection 4, and they do. The changes made to the aerosol land algorithm resulted in the improved comparison plots against AERONET for Collection 5 (see Figure 2). Overall mean AOD over land has decreased from 0.28 in Collection 4 to 0.19 in Collection 5. The land Collection 5 algorithm and comparison with Collection 4 is satisfactorily documented in the recent papers by Levy *et al.* [2007a, 2007b], and will not be further discussed here.

[30] The Collection 5 aerosol product that includes AOD over land and ocean, as well as indicators of aerosol particle size over land and ocean will be used to describe the global aerosol climatology. In section 4 and in the paragraphs above we have examined the validity of the aerosol optical depth (AOD) over land and ocean, and found the Collection 5 products accurate to within certain specified uncertainties. We have not examined the size parameters in the same manner. However, over ocean, we find the Collection 4 size parameters including fine mode fraction (FMF) to be well correlated with AERONET retrievals [Kleidman *et al.*, 2005]. Preliminary tests of Collection 5 particle size products over ocean demonstrate continued good correlation to AERONET values, with improved accuracy for coarse mode aerosols. The ocean FMF is a tested, well-understood product that delivers a quantitative measure of aerosol particle size and can be used with confidence for a variety of physical interpretations. In contrast, the land size parameter products are less certain. At best there is sufficient information in the land FMF for qualitative analysis on a global mean basis, and we do present such analysis in subsequent sections. However, we refrain from extending the analysis from global means to regional means, because while in some regions the FMF responds as expected, in other regions we are already aware that the land FMF is not properly representing seasonal transitions from one aerosol type to another [Jethva *et al.*, 2007]. Thus, we recommend to the community to freely use the FMF fraction over ocean, but to first evaluate the FMF over land for their particular application before including it in their analysis.

6. Global Mean Aerosol Optical Depth Over Ocean and Land

[31] Proceeding with Collection 5 we will now investigate the emerging global aerosol climatology as viewed by MODIS. Figure 5 shows the time series of monthly and global mean AOD through the MODIS record, which is of different length for Terra and Aqua. The data are separated by ocean and land retrievals, and by satellite. Over ocean the global mean AOD at 550 nm is 0.13 in Aqua and 0.14 in Terra, 10% of all ocean retrievals are below 0.041 in both satellites, but 10% are above 0.235 in Aqua while 10% are above 0.245 in Terra. The mean ocean AOD is close to the 66th percentile value, showing that the distribution is skewed toward lower values. The fine mode AOD, also plotted in Figure 5 follows the month by month variations of the total AOD. Mean fine mode AOD is approximately

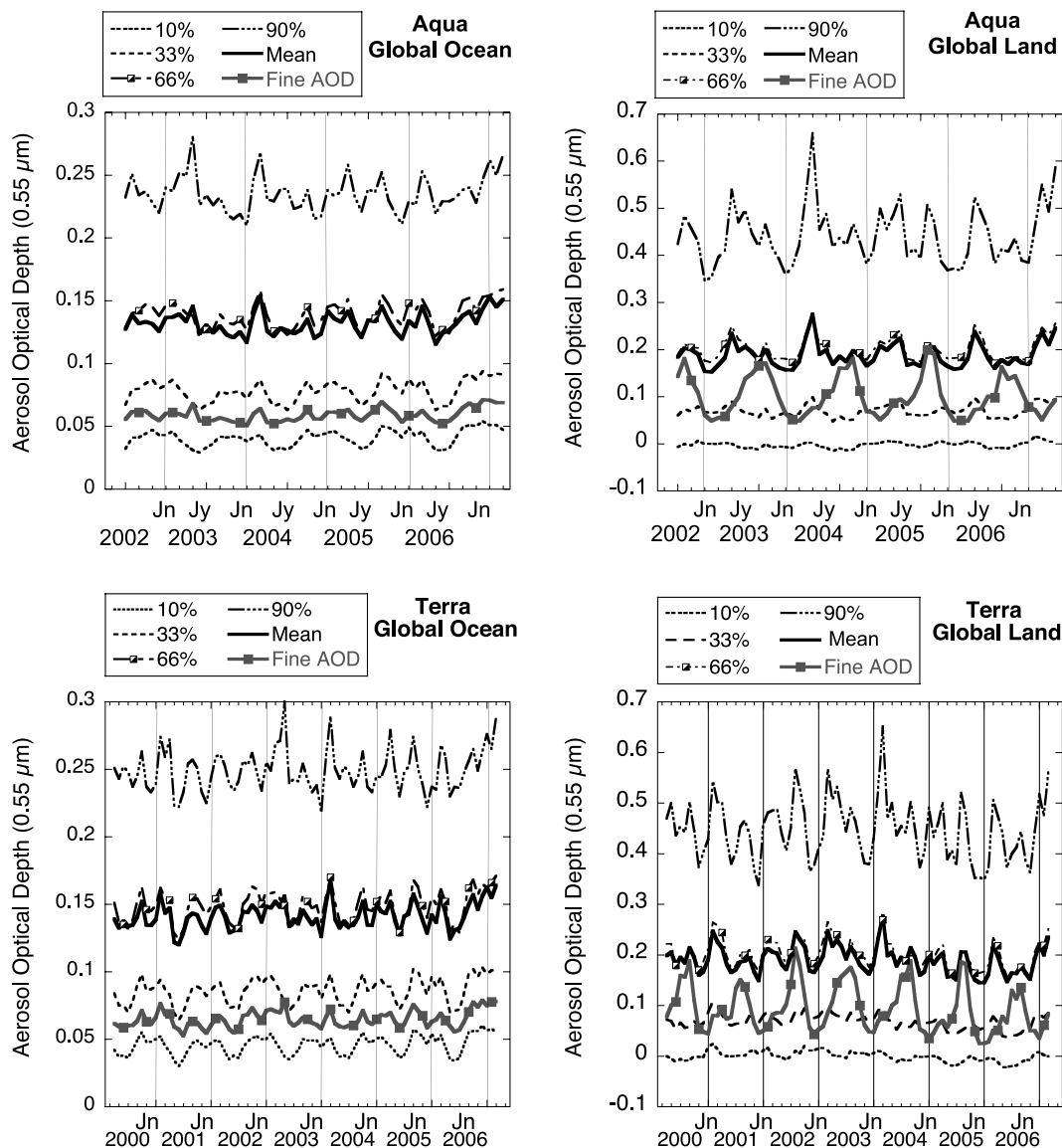


Figure 5. Time series of MODIS global aerosol optical depth at 550 nm (left) over ocean and (right) over land for (top) Aqua and (bottom) Terra. Monthly mean total AOD is plotted with a heavy black line. Contribution to the AOD from submicron particles is plotted in a heavy gray line. The percentile AODs are plotted by various dotted and dashed thin black lines. The mean AOD roughly corresponds to the 66% percentile over both ocean and land, showing that 66% of the monthly mean AOD values are less than the mean. Note that the vertical axes are different in the land and ocean plots.

0.06 in Aqua and 0.07 in Terra. Note that fine mode AOD contains fine mode contributions from marine aerosol and transported dust and pollution, and is thus not the same as the anthropogenic component.

[32] Over land the global mean AOD at 550 nm is 0.19, 10% of all land retrievals are negative and 10% are above 0.44, in both satellites. Note that the land retrieval permits negative AOD retrievals in order to avoid positive bias in the large-scale statistics [Levy *et al.*, 2007b]. The negative retrievals are confined to values $-0.05 < \text{AOD} < 0$ and are a recognition of the limited sensitivity of the algorithm to quantify the aerosol loading over land in very clean conditions. The meaning of the negative values is that there is no difference between small negative values, zero AOD or

small positive values. Approximately 20% of the AOD retrievals over land are of values too small for the instrument and algorithm to properly quantify. Over ocean the retrieval has greater sensitivity to small values of AOD and thus there are fewer (less than 2%) negative retrievals. The mean land AOD is also close to the 66th percentile showing the same skewed distribution as over ocean. The mean fine mode AOD is 0.10 in Aqua and 0.09 in Terra, which is larger than over ocean. Furthermore, over ocean we saw that fine mode AOD tracked with the total AOD month by month. Peaks in total AOD corresponded to peaks in fine mode AOD. Over land total AOD peaks in early spring, while fine mode AOD peaks in late summer and fall, during which fine mode AOD can account for almost the total

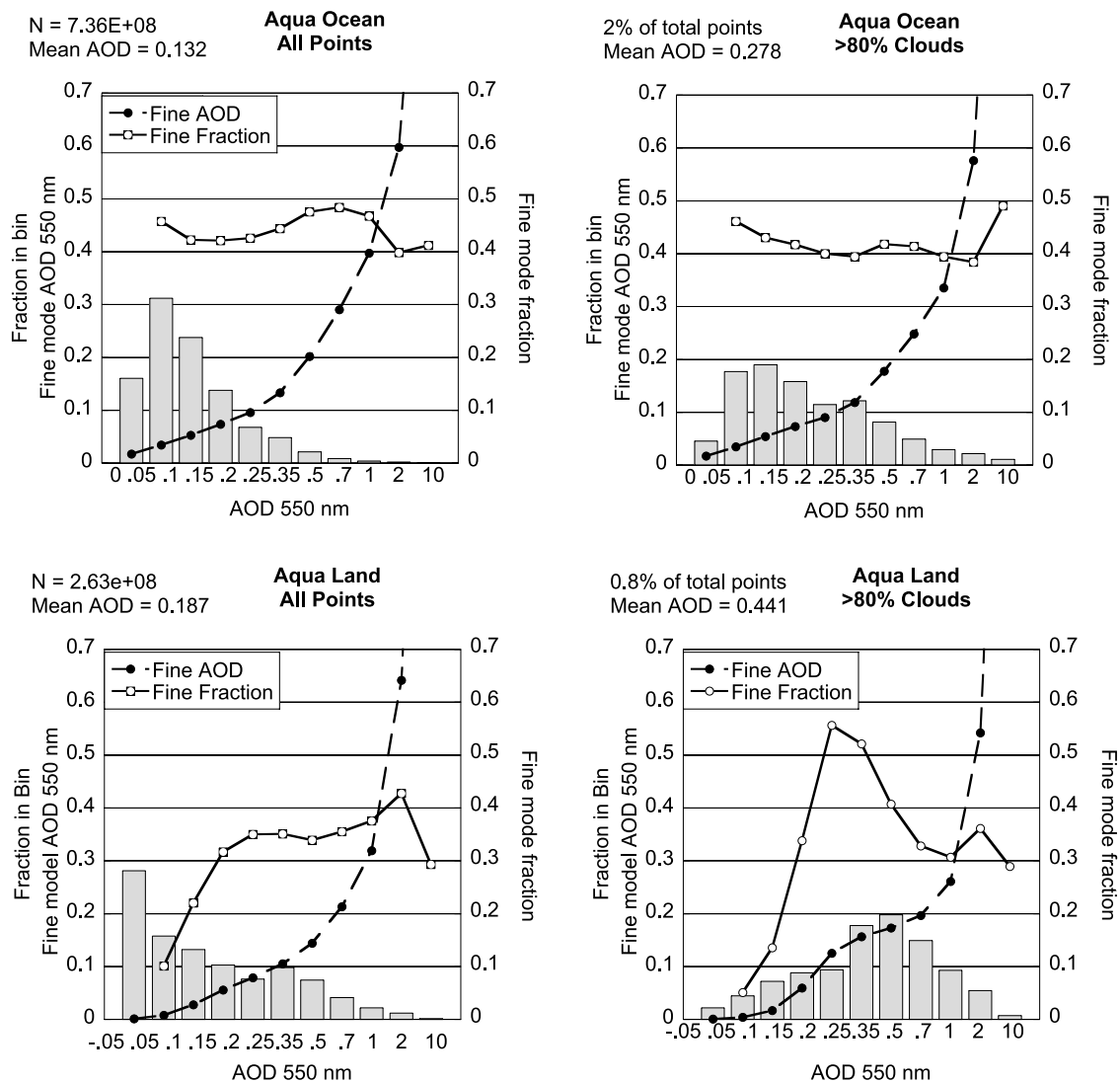


Figure 6. Aqua global aerosol optical depth histograms (AOD) over (top) ocean and (bottom) land constructed from daily $1^\circ \times 1^\circ$ latitude-longitude MODIS aerosol products, weighted by the number of 10 km retrievals in each 1° square. (left) Calculated from all available data. (right) Calculated only for those grid squares with greater than 80% cloud cover. Line with solid circles shows mean fine AOD in each total AOD bin. Line with open circles shows mean fine mode fraction (FMF) in each AOD bin. FMF is the fine AOD divided by the total AOD.

mean land AOD in that season. The seasonal cycles suggest a spring maximum due to dust transport and a fall maximum due to Southern Hemisphere biomass burning. However, there is a limit to the retrieval accuracy of aerosol size parameter over land. The fine mode AOD shown in the land plot of Figure 5 should be considered more of a qualitative indicator, rather than a validated quantitative product.

[33] Global mean values are strongly dependent on the way the data are aggregated averaged and weighted, and can vary by 20% or more. The statistics plotted in Figure 5 are calculated from QA-weighted L3 daily data weighted by the number of L2 retrievals, and are biased toward cloud free conditions. Although we acknowledge that aerosol in the vicinity of clouds may be different than far from clouds, aerosol “retrieval” near clouds may be contaminated in a

number of ways by the clouds themselves (3-D effects, subpixel cloud, etc). Thus, our choice of weighting by the number of L2 retrievals minimizes cloud effects on the aerosol statistics. Over ocean, this weighting leads to the lowest values of AOD global mean, whereas over land, the clear sky bias provides little difference.

7. Global AOD Statistics in the Vicinity of Clouds

[34] Figures 6 and 7 show the global mean statistics calculated from the L3 daily data directly without first creating monthly means, for the Aqua and Terra results, respectively. The global mean AOD values calculated from the histograms are the same as those calculated from the monthly means of Figure 5. Evident are the same skewed nature of the AOD distributions, and the broader range and

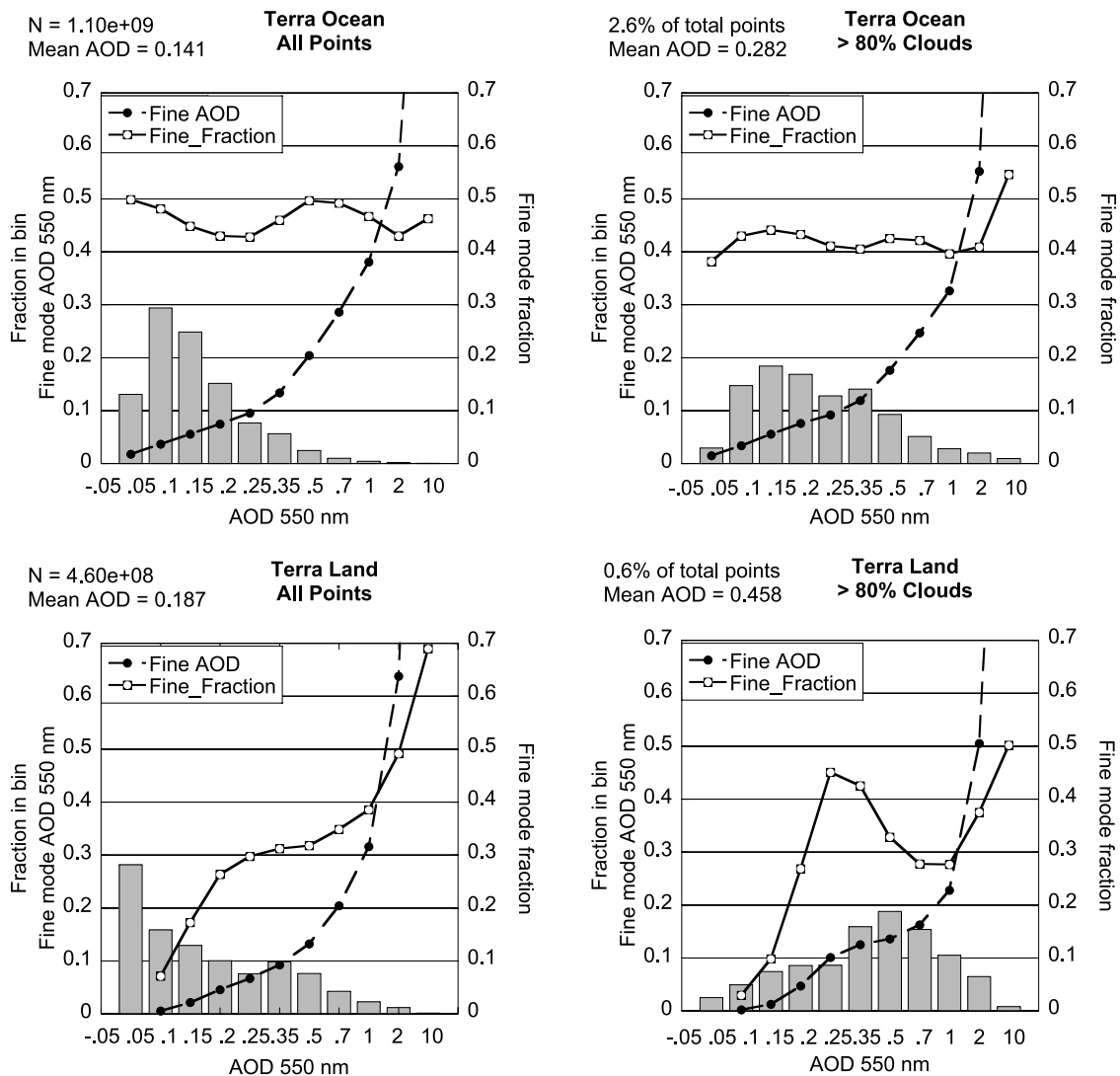


Figure 7. Same as Figure 6 but for Terra retrievals.

the negative values of the land histograms. In a global sense the fine mode fraction over ocean remains fairly constant over the range of ocean AOD values. Over land, however, the fine fraction suggests that coarse aerosol dominates at low AOD, transitioning to more equal partitioning at moderate AOD.

[35] The histogram analysis of Figures 6 and 7 permits examination of the effect of cloud fields on the aerosol statistics. Figures 6 and 7 (bottom) plot the AOD distributions for those grid squares in which the cloud fraction exceeds 80%. In these cloudy situations there is a drastic shift of AOD to higher values, both over ocean and land. The mean AOD for these cloudy situations approximately doubles to 0.28 over ocean and to 0.44–0.46 over land. We expect this increase in AOD to be in part caused by cloud contamination [Zhang *et al.*, 2005]. The aerosol retrieval would interpret cloud droplets in the field of view as being coarse mode particles. If subpixel clouds and other contaminants were the cause of the drastic increase in AOD in cloudy situations we would expect a strong decrease in fine mode fraction. There is some decrease in fine mode fraction

at moderate AOD over ocean, but not as much as would be expected from cloud contamination alone. Other factors including 3-D effects [Wen *et al.*, 2006, 2007] and increase of AOD from increased humidity around clouds [Koren *et al.*, 2007] are also possible explanations of the AOD increases. Such factors could help to explain the ocean results.

[36] Over land there is a sharp increase in fine mode fraction (FMF) at low to moderate values of AOD and a smaller decrease at high values of AOD. While cloud contamination is consistent for the AOD values over 0.5, the sharp increase in FMF at lower AOD may be explained by either 3-D effects or increases of humidity fields around clouds in these cloudy land scenes. However, we cannot rule out a sampling artifact in which 80% cloud fraction situations may be associated with meteorology that has higher concentrations of a fine mode aerosol type. For example, in the eastern United States, high-pollution episodes in the summer are associated with stagnant meteorological conditions and boundary cumulus cloud fields [Kaufman *et al.*, 2002]. Also the small number of statistics

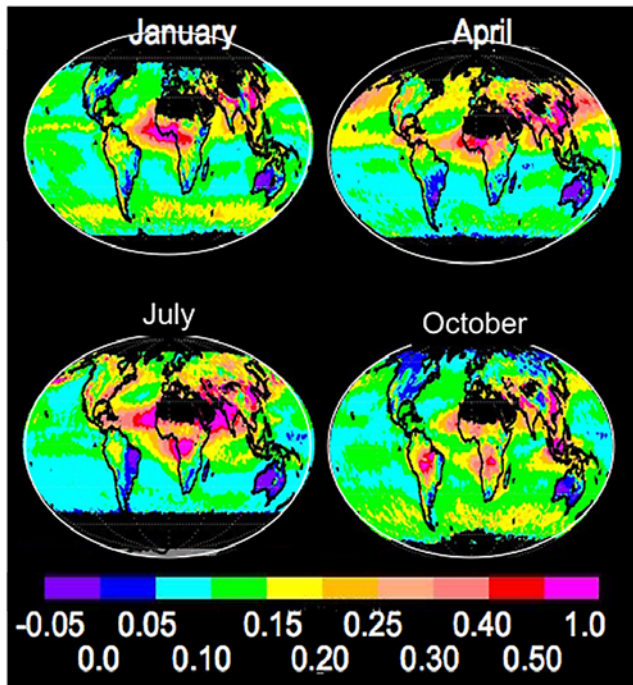


Figure 8. Five year mean global distribution of aerosol optical depth (AOD) at 550 nm for four selected months: January, April, July, and October. The averages were calculated from daily $1^\circ \times 1^\circ$ latitude-longitude MODIS aerosol products, weighted by the number of L2 retrievals in the grid square. Negative values in purple identify where AOD is so low that it cannot be distinguished from zero. Black indicates fill value where no retrieval was attempted. Retrievals are not attempted over snow, during polar night, or over bright deserts.

in the $> 80\%$ plots can be easily influenced by sampling biases. Note that the cloudy situations in Figures 6 and 7 represent only 2% of the total number of grid squares included in the overall statistics over ocean and less than 1% over land.

8. Regional and Seasonal Distribution of Aerosol Optical Depth

[37] Up to this point we have analyzed the global aerosol system in terms of its global mean statistics. The aerosol system is far from being well mixed and homogenous. The aerosol story is very much linked to geography and season. Figure 8 shows 4 months of aerosol optical depth observed from Aqua MODIS. The 4 months were chosen to represent seasonal changes, and each month is the mean of that month over the 5 years of the Aqua mission. In Figure 8 we see the strong aerosol loading over eastern China, the Indo-Gangetic Plain of India and in the eastern tropical north Atlantic during all seasons. We see the aerosol from biomass burning in Africa in January north of the equator shift southward during the course of the year until it is joined by tropical biomass burning in the Amazon and Indonesia during northern autumn. There is wide spread

elevated AOD over the oceans during the spring of each hemisphere, April in the north and October in the south. During northern summer the Arabian Sea and India exhibit unusually high AOD values, while North America, Europe and northern Asia have their highest, though moderate, aerosol loading during the same season.

[38] Figure 8 also shows the limits of the MODIS aerosol products to represent the global aerosol system. Large expanses of the globe are left blank during various seasons because of polar night or surfaces unsuitable for making a dark target retrieval. The new Deep Blue product will fill in some of these spaces when combined with the standard aerosol products although that prospect is outside the scope of this study. Because of these missing regions, the global mean aerosol values described here may not be truly representative of the entire globe, particularly over land. Other sampling considerations, including biases to cloud free conditions and no ocean retrievals over sun glint, affect the ability of a satellite monthly mean to represent the entire month at any particular grid square. Still, a comprehensive picture does emerge from the statistics of satellite data sets.

9. Aerosol Optical Depth of Individual Regions

[39] We define 13 regions over ocean (following Remer and Kaufman [2006]) and 14 regions over land to examine MODIS-derived aerosol characteristics in greater detail. Figures 9 and 10 define these regions. Seasonal and annual mean AOD for each region are plotted in Figures 9 and 10, and the seasonal and annual mean fine mode fraction (FMF) is also plotted for each region in Figure 9. While biases between Terra and Aqua AOD were noted above, the aerosol products from the two satellites exhibit nearly identical seasonal and regional patterns. Thus, for brevity only values from Aqua are plotted in Figure 9. Table 1 gives the numerical values for ocean regions and Table 2 for land, for both satellites. The heaviest aerosol loading can be found over India and the surrounding oceans during northern summer (JJA). East Asia also exhibits heavy aerosol loading, but during northern spring (MAM). The southern tropical Pacific shows the lowest oceanic AOD, but MODIS-observed AOD over the Australian continent is even lower, although the Australian values fall within the land algorithm's noise level.

[40] Because the seasonal cycle is most pronounced near the aerosol source regions over land we concentrate our seasonal analysis on the land regions. Figure 11 shows the AOD time series from Aqua for four categories of regions: northern industrial economies, southern biomass burning regions, dust dominated and Asia. The four regions grouped as northern industrial economies are west and east North America, north Europe and the Mediterranean Basin. These four regions track together exhibiting increased AOD in the spring and summer, but only to moderate levels as compared to other regions of the globe. The fall and winter seasons have very low AOD with eastern North America surprisingly showing the lowest values of AOD during the winter. The Mediterranean region, which includes parts of North Africa and the Middle East as well as southern Europe has a longer aerosol season with higher AOD values both in summer and in winter than the other three regions.

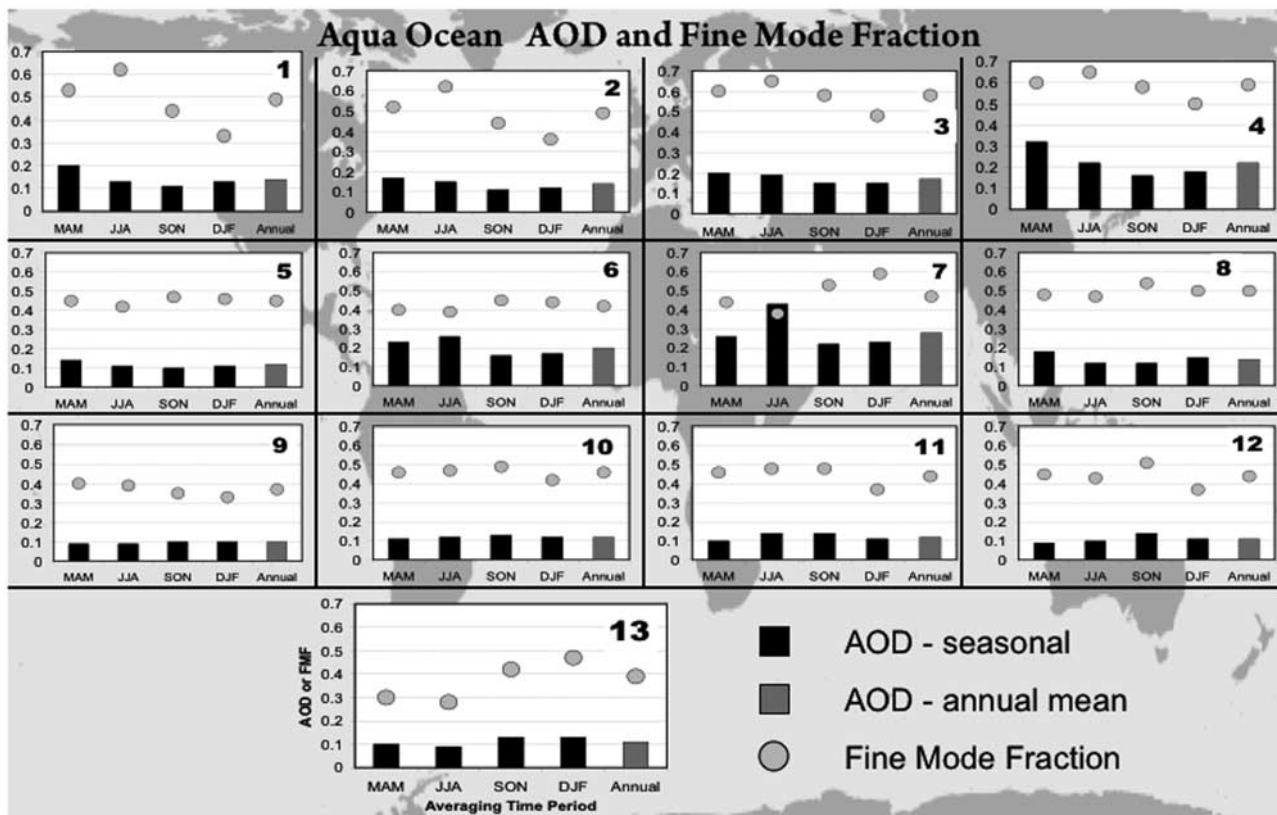


Figure 9. Seasonal and annual mean AOD at 550 nm and fine mode fraction (FMF) for 13 ocean regions for the Aqua satellite. Seasonal mean AOD is shown by black columns, annual mean is shown by gray columns, and FNF is shown by gray dots. The 13 bar graphs are positioned onto a map of the globe, corresponding to the area used in defining that region. Data for the bar graphs are given explicitly in Table 1.

[41] The three southern biomass burning regions, South America, southern Africa and Indonesia, show very similar seasonal patterns, despite their widely varying locations. The biomass burning season in the Southern Hemisphere occurs during southern spring (SON) on all three continents. There is a high degree of interannual variability in the AOD values at each location. The AOD during the biomass burning season is roughly twice the AOD values of the northern industrial economies, excluding the Mediterranean. However, during the 3/4 of the year with no burning, South America and southern Africa have low AOD comparable with values in North America and northern Europe.

[42] Northern Africa and India, grouped together because both are affected by dust transported from the Sahara and Arabia, have overall higher AOD than any of the previous regions. North Africa exhibits an irregular seasonal cycle with the highest values reported in later winter (February and March) at the peak of the Northern Hemisphere biomass burning season, but there is an irregular extension of the high AOD season that extends into late summer when dust is dominant. India's seasonal cycle is more regular with a broad aerosol season spanning the period March to July. In 2006 only, we see a suggestion of a second aerosol season occurring that winter.

[43] The fourth grouping of regions in Figure 11 are the Asian regions, excluding India and Indonesia, which were previously discussed. The Asian regions include Siberia, east Asia, which is mainly China, and Southeast Asia. The AOD values in Siberia are low, especially in autumn and winter. However, snow covers much of the region in winter and therefore, MODIS does not sample much of this region in that season. Summer AOD values in Siberia are comparable to summer values in North America and northern Europe. Note that Siberia seems to track with the Asian regions to the south, although at much lower aerosol loading. This suggests some commonality in aerosol transport or similarity of sources. East Asia and Southeast Asia track together showing an extended aerosol season that spans the spring and summer seasons. The AOD during the aerosol season shows interannual variability for both regions that can exceed values from the dust regions of northern Africa, India or the Southern Hemisphere biomass burning regions. AOD values remain moderately high even for the autumn and winter months.

10. Aerosol Size Characteristics of Individual Regions

[44] Aerosol particle size can be described by a variety of parameters in the MODIS aerosol data product including

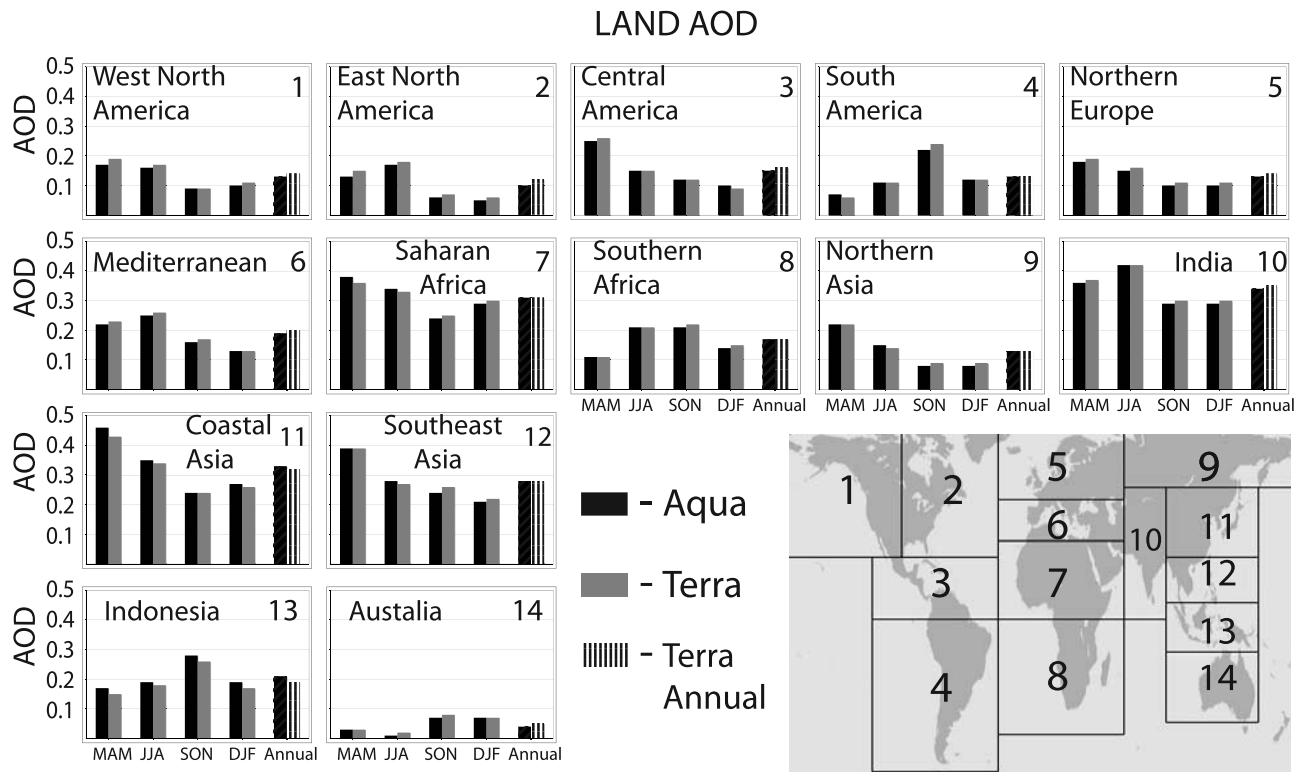


Figure 10. Seasonal and annual mean AOD for 14 land regions defined at bottom right. Terra AOD shown by black columns and Aqua AOD is shown with gray columns. The column in the far right for each regional bar graph denotes the annual mean. The seasonal means from left to right in each regional bar graph are MAM, JJA, SON, and DJF. Dates for the bar graphs are given explicitly in Table 2.

Table 1. Seasonal and Annual Aerosol Optical Depth at 550 nm and Fine Mode Fraction for Each Ocean Region of Figure 9^a

	MAM		JJA		SON		DJF		Annual	
	AOD	FMF	AOD	FMF	AOD	FMF	AOD	FMF	AOD	FMF
<i>Aqua: 5 Year Means</i>										
NE Pacific	0.20	0.53	0.13	0.62	0.11	0.44	0.13	0.33	0.14	0.49
North Atlantic	0.17	0.52	0.15	0.62	0.11	0.44	0.12	0.36	0.14	0.49
Mediterranean	0.20	0.60	0.19	0.65	0.15	0.58	0.15	0.48	0.17	0.58
NW Pacific	0.32	0.60	0.22	0.65	0.16	0.58	0.18	0.50	0.22	0.59
Tropical NE Pacific	0.14	0.45	0.11	0.42	0.10	0.47	0.11	0.46	0.12	0.45
Tropical North Atlantic	0.23	0.40	0.26	0.39	0.16	0.45	0.17	0.44	0.20	0.42
North Indian	0.26	0.44	0.43	0.38	0.22	0.53	0.23	0.59	0.28	0.47
Tropical NW Pacific	0.18	0.48	0.12	0.47	0.12	0.54	0.15	0.50	0.14	0.50
Tropical SE Pacific	0.09	0.40	0.09	0.39	0.10	0.35	0.10	0.33	0.10	0.37
Tropical South Atlantic	0.11	0.46	0.12	0.47	0.13	0.49	0.12	0.42	0.12	0.46
South Indian	0.10	0.46	0.14	0.48	0.14	0.48	0.11	0.37	0.12	0.44
Tropical SW Pacific	0.09	0.45	0.10	0.43	0.14	0.51	0.11	0.37	0.11	0.44
South circumpolar	0.10	0.30	0.09	0.28	0.13	0.42	0.13	0.47	0.11	0.39
<i>Terra: 7 Year Means</i>										
NE Pacific	0.21	0.50	0.15	0.63	0.12	0.41	0.13	0.28	0.15	0.45
North Atlantic	0.18	0.51	0.16	0.63	0.12	0.42	0.13	0.34	0.15	0.47
Mediterranean	0.21	0.58	0.20	0.67	0.17	0.57	0.14	0.48	0.18	0.57
NW Pacific	0.34	0.56	0.23	0.67	0.16	0.56	0.19	0.46	0.23	0.56
Tropical NE Pacific	0.16	0.53	0.12	0.49	0.11	0.51	0.12	0.48	0.13	0.50
Tropical North Atlantic	0.23	0.44	0.26	0.40	0.17	0.47	0.18	0.43	0.21	0.44
North Indian	0.27	0.49	0.43	0.37	0.24	0.57	0.24	0.61	0.29	0.51
Tropical NW Pacific	0.18	0.53	0.10	0.52	0.13	0.56	0.15	0.51	0.15	0.53
Tropical SE Pacific	0.10	0.46	0.09	0.40	0.11	0.40	0.11	0.42	0.10	0.42
Tropical South Atlantic	0.11	0.50	0.12	0.47	0.15	0.51	0.14	0.46	0.13	0.49
South Indian	0.11	0.50	0.14	0.47	0.15	0.52	0.12	0.46	0.13	0.49
Tropical SW Pacific	0.10	0.50	0.11	0.45	0.16	0.54	0.12	0.45	0.12	0.49
South circumpolar	0.11	0.29	0.10	0.24	0.15	0.38	0.14	0.47	0.12	0.35

^aAOD, aerosol optical depth; FMF, fine mode fraction.

Table 2. Seasonal and Annual Aerosol Optical Depth at 550 nm for Each Land Region of Figure 10

	MAM	JJA	SON	DJF	Annual
<i>Aqua: 5 Year Means</i>					
West North America	0.17	0.16	0.09	0.10	0.13
East North America	0.13	0.17	0.06	0.05	0.10
Central America	0.25	0.15	0.12	0.10	0.15
South America	0.07	0.11	0.22	0.12	0.13
North Europe	0.18	0.15	0.10	0.10	0.13
Mediterranean Basin	0.22	0.25	0.16	0.13	0.19
North Africa	0.38	0.34	0.24	0.29	0.31
South Africa	0.11	0.21	0.21	0.14	0.17
Siberia	0.22	0.15	0.08	0.08	0.13
India	0.36	0.42	0.29	0.29	0.34
East Asia	0.46	0.35	0.24	0.27	0.33
SE Asia	0.39	0.28	0.24	0.21	0.28
Indonesia	0.17	0.19	0.28	0.19	0.21
Australia	0.03	0.01	0.07	0.07	0.04
<i>Terra: 7 Year Means</i>					
West North America	0.19	0.17	0.09	0.11	0.14
East North America	0.15	0.18	0.07	0.06	0.12
Central America	0.26	0.15	0.12	0.09	0.16
South America	0.06	0.11	0.24	0.12	0.13
North Europe	0.19	0.16	0.11	0.11	0.14
Mediterranean Basin	0.23	0.26	0.17	0.13	0.20
North Africa	0.36	0.33	0.25	0.30	0.31
South Africa	0.11	0.21	0.22	0.15	0.17
Siberia	0.22	0.14	0.09	0.09	0.13
India	0.37	0.42	0.30	0.30	0.35
East Asia	0.43	0.34	0.24	0.26	0.32
SE Asia	0.39	0.27	0.26	0.22	0.28
Indonesia	0.15	0.18	0.26	0.17	0.19
Australia	0.03	0.02	0.08	0.07	0.05

fine mode AOD, fine mode fraction and various Angstrom Exponents. These parameters provide subtle differences, but are more or less correlated with each other. The ocean algorithm uses 6 wavelengths and benefits from a fairly homogenous background surface. Therefore, the ocean product contains inherently greater information content than the land product, which uses only three wavelengths and is sensitive to the assumptions made about the spectral surface reflectance. In essence, the size parameters from the ocean algorithm are more reliable than the land. We are already aware of specific regions where the land size parameter is systematically wrong [Jethva *et al.*, 2007] and prefer to wait until full characterization of the land size parameter is available before calculating regional climatological statistics. In the regional analysis we focus the size parameter analysis solely on the ocean retrievals.

[45] Table 1 shows the seasonal and annual mean fine mode fraction (FMF) for the 13 ocean regions. Values range from 0.28 to 0.35 in pristine Southern Hemisphere regions to 0.60–0.65 in the northern midlatitudes. These seasonal mean numbers conform to our expectations that pristine oceanic regions would be dominated by sea salt, a coarse mode aerosol, and therefore have smaller FMF, while northern midlatitudes would have a greater fine mode contribution from aerosol transported from land sources.

[46] We obtain greater physical interpretation by plotting monthly mean aerosol size parameter against monthly mean total AOD, following Kaufman *et al.* [2005]. For this exercise we chose to use the fine AOD rather than FMF because it produces higher correlations and a clearer picture. At low AOD, FMF, which is a ratio of two small numbers

can be noisy. On the other hand, fine AOD becomes smaller as total AOD becomes smaller, and is less noisy. Figure 12 shows the results for five regions using Aqua data. The results fall into two classes. Regions 2, 4, and 13 fall into the first class. In this situation, as aerosol optical depth is added to a baseline background value, AOD of the fine mode increases as well. The slopes of the linear regression fits are approximately in the range of 0.7–0.8. Region 6 represents the second class. Here fine AOD also increases as total AOD increases, but at a much slower rate. The slope of the class 2 regression is approximately 0.3. We interpret these two classes as the difference between adding smoke/pollution to a background marine aerosol in which the slope is the higher value, and adding dust, which results in the smaller slope.

[47] We expect elevated AOD in region 2 to be pollution from North America and Europe. Likewise we expect elevated AOD in region 6 to be dust from the Sahara. However, it is somewhat surprising that the elevated aerosol in region 13 follows the smoke/pollution curve so tightly. This suggests that elevated aerosol in the southern circumpolar ocean has a strong biomass burning component, and indeed the seasonal means in Table 1 shows that elevated AOD and FMF occur during the Southern Hemisphere biomass burning season. We also expected that some of the elevated aerosol in region 4 would have a dust component from transported Asian dust. Instead we see a tight correlation following the smoke/pollution curve. Figure 12 also plots region 7, the northern Indian Ocean, which splits its monthly means to follow both curves. This suggests that in some months the aerosol is dust and other months it is smoke/pollution. The results from Terra are similar to Aqua, and thus Figure 12 shows only Aqua to avoid redundancy.

[48] Table 3 gives several annual mean aerosol size parameters, and the regression slope and correlation coefficients following Figure 12 for each ocean region, for both satellites. Note that regions 3, 7, and 9 have small slopes and relatively low R^2 values. A low R^2 gives indication that the region follows neither class. In some cases this is because some months follow the smoke/pollution curve and other months the dust curve (regions 3 and 7), but in other cases the region remains pristine through all months and there is no elevated aerosol (region 9).

11. Discussion and Conclusions

[49] The MODIS aerosol product derived from 7 years of Terra data and 5 years of Aqua data has recently undergone reprocessing using a new algorithm labeled Collection 5. Collection 5 represents both new aerosol algorithm and new calibration coefficients, applied consistently through the entire data records of each MODIS sensor. Comparison of Collection 5 MODIS aerosol optical depth (AOD) retrievals over ocean and land with high-quality AERONET observations shows agreement as good as Collection 4 for ocean and much improved for land. In fact, in Collection 5 the land algorithm is retrieving AOD at midvisible wavelengths as accurately as the ocean algorithm, with similar or smaller offsets, regression slopes close to 1.0 and similar or better correlation. Comparison with collocated AERONET products requires both MODIS and AERONET to report cloud free conditions. Situations where MODIS retrieves but

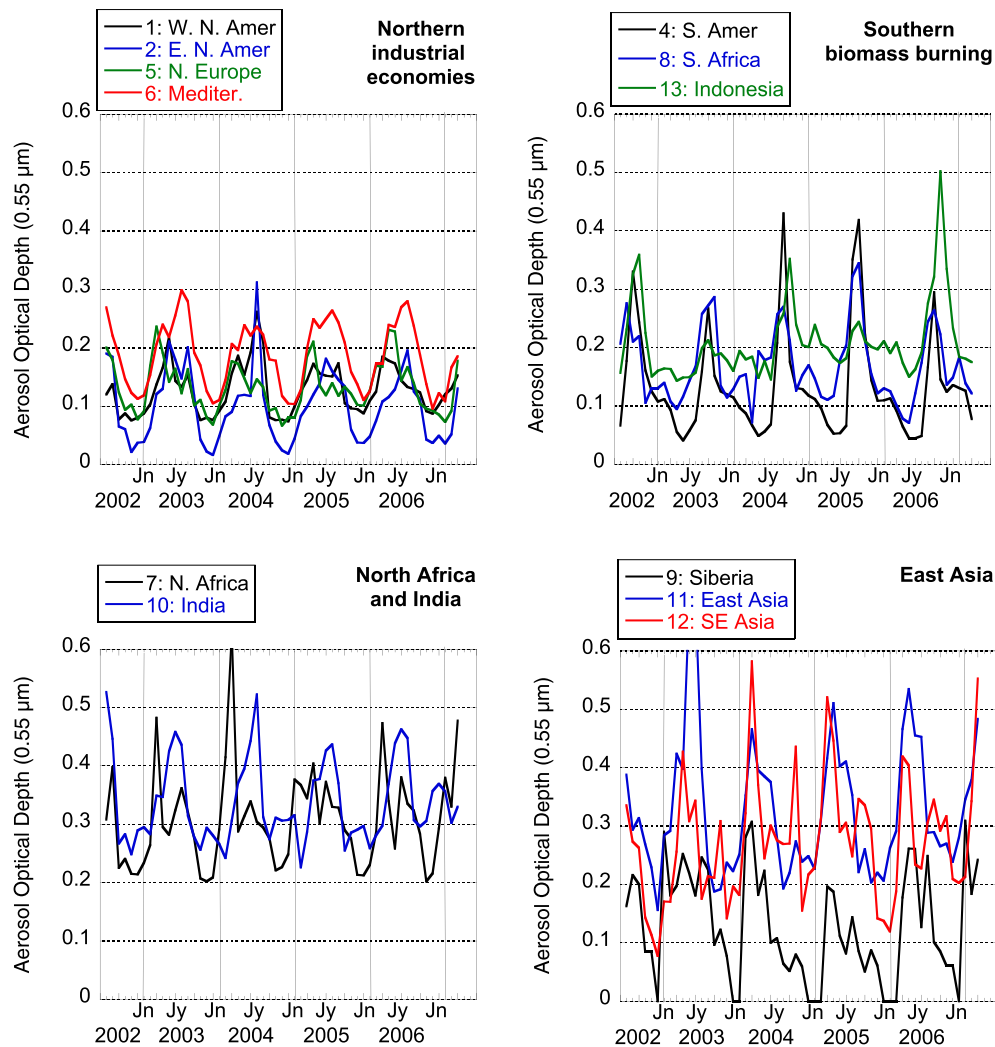


Figure 11. Time series of Aqua regional monthly mean aerosol optical depth (AOD) over land at 550 nm calculated from daily $1^\circ \times 1^\circ$ latitude-longitude MODIS aerosol products weighted by the number of L2 retrievals in the grid square. Regions are defined in Figure 10. Terra regional monthly mean AOD follow similar seasonal patterns as Aqua and are not shown.

AERONET does not were not included in the analysis. Validation efforts continue, and a more comprehensive validation study is in preparation.

[50] The differences we expected to find between Collection 4 and Collection 5 included a shift to larger particle sizes over ocean but no change to ocean AOD. In the Aqua record, indeed that is exactly what we find. However, something else has occurred in the Terra record, as not only did the Terra ocean particle size shift, but its global mean ocean AOD was larger by 0.015. The MODIS aerosol software is applied equally to Terra and Aqua. To apply the same algorithm and have Terra oceanic AOD shift by 0.015, while Aqua AOD remain the same is impossible. The only logical answer is that MODIS calibration constants also changed between Collections. Indeed adjustments were made to the calibration coefficients of the seven MODIS wavelengths used by the aerosol algorithm during the Collection 5 reprocessing. Terra's coefficients were adjusted up to 2% depending on wavelength, while adjustments to

Aqua's coefficients were less than 0.5% (MODIS Characterization Science Team, personal communication, 2007).

[51] We have presented an analysis of MODIS aerosol optical depth and particle size information, over ocean and land, globally and regionally. We have shown time series and histograms. From this analysis we conclude the following:

[52] 1. Global mean AOD is 0.13 to 0.14 over ocean and 0.19 over land. The range over ocean reflects the differences between Terra and Aqua AOD statistics.

[53] 2. Terra and Aqua, despite the offset in ocean AOD statistics, show similar regional and seasonal variation, and similar mean values over land. Real diurnal aerosol differences cannot be discerned above the products' uncertainties at this time.

[54] 3. At every decision point in the processing we have taken the road leading to lower values of global mean AOD. In particular by weighting each grid square in the aggregation by the number of L2 retrievals in that square, the ocean

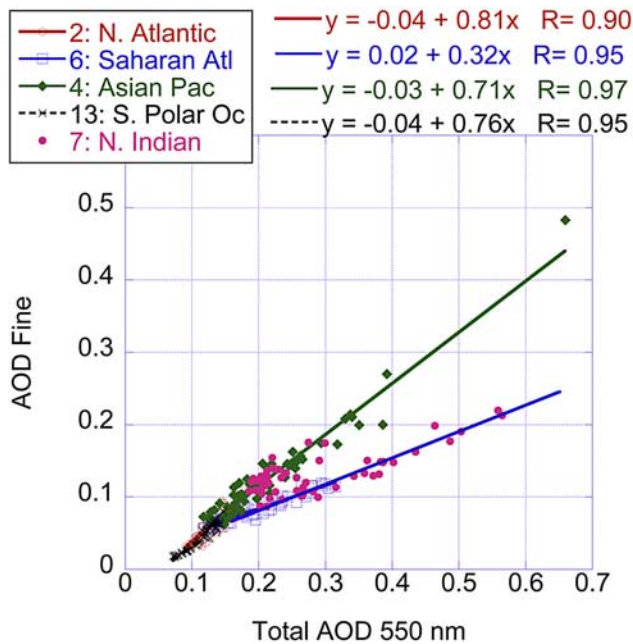


Figure 12. Aqua monthly and regional mean fine AOD over ocean plotted against monthly and regional mean total AOD for five selected ocean regions. Regression lines and correlations are calculated and displayed. Regions fall into two classes defined by the slope of this regression. Most regions have slopes in the 0.7 to 0.8 range, as demonstrated by region 4 (NW Pacific) and denoted by the green line. However, region 6 (north tropical Atlantic) has a slope of 0.32 and is denoted by the blue line. Region 7 (North Indian Ocean) has a seasonal shift with the months of October through March following the green line and months April through September following the blue line.

global mean AOD is lower by 0.03 than if calculated without this weighting.

[55] 4. We feel that the higher range of values that would be achieved without L2 weighting contain cloud artifacts. Therefore we decided to produce values that are least affected by clouds and are at the lower range of the envelope.

[56] 5. Land shows a broader distribution of AOD than ocean. Roughly 28% of land retrievals are extremely clean and within ± 0.05 of $\text{AOD} = 0$. Only 15% of ocean retrievals are that low.

[57] 6. Global mean values are limited by sampling issues. No retrievals are made during polar night, snow, ice or bright land surfaces, or when clouds cover the scene.

[58] 7. Global mean values can vary by as much as 20% depending on how the data is aggregated, weighted and averaged. The results here are L2 weighted. Thus, they are biased to clear skies and the reported AOD may be low.

[59] 8. AOD in situations with 80% cloud fraction are twice the global mean values, although such situations occur only 2% of the time over ocean and less than 1% of the time over land.

[60] 9. There is no drastic change in aerosol particle size associated with these very cloudy situations over ocean, but there appears to be a large shift over land.

[61] 10. The heaviest aerosol regions are North Africa, India, east and Southeast Asia. Each has its own seasonal cycle and interannual variability.

[62] 11. The northern industrial economies (North America and Europe), Siberia and especially Australia have the lowest average AODs.

[63] 12. The three Southern Hemisphere biomass burning regions (South America, southern Africa and Indonesia) exhibit very similar seasonal behavior.

[64] 13. We find that in most oceanic regions elevated aerosol over background conditions is dominated by fine mode aerosol and not dust. This includes the Mediterranean, the north Pacific downwind of Asia and even the southern oceans. Only the Saharan outflow region in the Atlantic and the Arabian Sea area have certain months dominated by dust.

[65] We demonstrate in this work an emerging climatology of aerosol characteristics using the satellite view from MODIS. Longer records are necessary to fully characterize trends and further analysis with multiple data sets is necessary to better unravel the signatures of aerosols and clouds. However, this view from space and “checkup” of the aerosol system provides valuable information for understanding the planet now and estimating the potential consequences of global change.

Table 3. Annual Mean Aerosol Optical Depth at 550 nm, Fine Mode AOD, Fine Mode Fraction, Angstrom Exponent Defined by 550 nm and 870 nm, Slope of the Regression Between AOD Fine and AOD, and Correlation of the Regression^a

Region	AOD	AOD Fine	FMF	Ang1	Slope	R ²
<i>Aqua</i>						
NE Pacific	0.14	0.07	0.49	0.65	0.72	0.79
North Atlantic	0.14	0.07	0.49	0.66	0.81	0.80
Mediterranean	0.17	0.1	0.58	0.87	0.69	0.77
NW Pacific	0.22	0.13	0.59	0.84	0.71	0.94
Tropical NE Pacific	0.12	0.05	0.45	0.60	0.49	0.83
Tropical North Atlantic	0.20	0.09	0.42	0.52	0.32	0.90
North Indian	0.28	0.13	0.47	0.65	0.22	0.58
Tropical NW Pacific	0.14	0.07	0.50	0.67	0.57	0.84
Tropical SE Pacific	0.10	0.04	0.37	0.45	0.30	0.40
Tropical South Atlantic	0.12	0.06	0.46	0.60	0.64	0.81
South Indian	0.12	0.06	0.44	0.59	0.70	0.88
Tropical SW Pacific	0.11	0.05	0.44	0.59	0.65	0.83
South circumpolar	0.11	0.04	0.39	0.44	0.76	0.91
<i>Terra</i>						
NE Pacific	0.15	0.07	0.45	0.58	0.70	0.73
North Atlantic	0.15	0.07	0.47	0.61	0.85	0.77
Mediterranean	0.18	0.10	0.57	0.81	0.76	0.79
NW Pacific	0.23	0.13	0.56	0.76	0.67	0.88
Tropical NE Pacific	0.13	0.06	0.50	0.62	0.63	0.90
Tropical North Atlantic	0.21	0.09	0.44	0.50	0.34	0.88
North Indian	0.29	0.14	0.51	0.62	0.14	0.36
Tropical NW Pacific	0.15	0.08	0.53	0.67	0.63	0.87
Tropical SE Pacific	0.10	0.04	0.42	0.48	0.41	0.59
Tropical South Atlantic	0.13	0.06	0.49	0.60	0.59	0.81
South Indian	0.13	0.06	0.49	0.60	0.62	0.89
Tropical SW Pacific	0.12	0.06	0.49	0.62	0.68	0.92
South circumpolar	0.12	0.04	0.35	0.37	0.71	0.84

^aAOD, aerosol optical depth; FMF, fine mode fraction.

[66] **Acknowledgments.** This work was first put in motion almost 3 years ago by our coauthor, mentor, and dear friend, Yoram Kaufman. We miss Yoram's guidance and inspiration almost every single day. The three anonymous reviewers gave us constructive suggestions that improved the paper significantly, and we thank them. We also wish to acknowledge the many AERONET PIs and their site managers who make the AERONET program possible. The research was supported by NASA's Radiation Sciences Program and Earth Observation System Project Office.

References

- Ackerman, S. A., K. I. Strabala, W. P. Menzel, R. A. Frey, C. C. Moeller, and L. E. Gumley (1998), Discriminating clear sky from clouds with MODIS, *J. Geophys. Res.*, *103*, 32,141–32,157, doi:10.1029/1998JD200032.
- Anderson, T. L., R. J. Charlson, D. M. Winker, J. A. Ogren, and K. Holmén (2003), Mesoscale variations of tropospheric aerosols, *J. Atmos. Sci.*, *60*, 119–136, doi:10.1175/1520-0469(2003)060<0119:MVOTA>2.0.CO;2.
- Chu, D. A., Y. J. Kaufman, L. Remer, and B. N. Holben (1998), Remote sensing of smoke from MODIS Airborne Simulator during the SCAR-B Experiment, *J. Geophys. Res.*, *103*, 31,979–31,987.
- Chu, D. A., Y. J. Kaufman, C. Ichoku, L. A. Remer, D. Tanré, and B. N. Holben (2002), Validation of MODIS aerosol optical depth retrieval over land, *Geophys. Res. Lett.*, *29*(12), 8007, doi:10.1029/2001GL013205.
- d'Almeida, G. A., P. Koepke, and E. P. Shettle (1991), *Atmospheric Aerosols: Global Climatology and Radiative Characteristics*, A. Deepak, Hampton, Va.
- Dubovik, O., and M. D. King (2000), A flexible inversion algorithm for retrieval of aerosol optical properties from Sun and sky radiance measurements, *J. Geophys. Res.*, *105*, 20,673–20,696.
- Dubovik, O., B. N. Holben, T. F. Eck, A. Smirnov, Y. J. Kaufman, M. D. King, D. Tanré, and I. Slutsker (2002), Variability of absorption and optical properties of key aerosol types observed in worldwide locations, *J. Atmos. Sci.*, *59*, 590–608, doi:10.1175/1520-0469(2002)059<0590:VOAAP>2.0.CO;2.
- Eck, T. F., B. N. Holben, J. S. Reid, O. Dubovik, A. Smirnov, N. T. O'Neill, I. Slutsker, and S. Kinne (1999), Wavelength dependence of the optical depth of biomass burning, urban and desert dust aerosols, *J. Geophys. Res.*, *104*, 31,333–31,350.
- Gao, B.-C., Y. J. Kaufman, D. Tanré, and R.-R. Li (2002), Distinguishing tropospheric aerosols from thin cirrus clouds for improved aerosol retrievals using the ratio of 1.38- μm and 1.24- μm channels, *Geophys. Res. Lett.*, *29*(18), 1890, doi:10.1029/2002GL015475.
- Geogdzhayev, I. V., M. I. Mishchenko, W. B. Rossow, B. Cairns, and A. A. Lacis (2002), Global two-channel AVHRR retrievals of aerosol properties over the ocean for the period of NOAA-9 observations and preliminary retrievals using NOAA-7 and NOAA-11 data, *J. Atmos. Sci.*, *59*, 262–278, doi:10.1175/1520-0469(2002)059<0262:GTCARO>2.0.CO;2.
- Geogdzhayev, I. V., M. I. Mishchenko, E. I. Terez, G. A. Terez, and G. K. Gushchin (2005), Regional advanced very high resolution radiometer-derived climatology of aerosol optical thickness and size, *J. Geophys. Res.*, *110*, D23205, doi:10.1029/2005JD006170.
- Holben, B. N., et al. (1998), AERONET-A federated instrument network and data archive for aerosol characterization, *Remote Sens. Environ.*, *66*, 1–16, doi:10.1016/S0034-4257(98)00031-5.
- Holben, B. N., et al. (2001), An emerging ground-based aerosol climatology: Aerosol optical depth from AERONET, *J. Geophys. Res.*, *106*, 12,067–12,097.
- Hsu, N. C., S. C. Tsay, M. D. King, and J. R. Herman (2004), Aerosol properties over bright-reflecting source regions, *IEEE Trans. Geosci. Remote Sens.*, *42*, 557–569, doi:10.1109/TGRS.2004.824067.
- Husar, R. B., J. M. Prospero, and L. L. Stowe (1997), Characterization of tropospheric aerosols over the oceans with the NOAA advanced very high resolution radiometer optical thickness operational product, *J. Geophys. Res.*, *102*, 16,889–16,910, doi:10.1029/96JD04009.
- Ichoku, C., D. A. Chu, S. Mattoo, Y. J. Kaufman, L. A. Remer, D. Tanré, I. Slutsker, and B. N. Holben (2002), A spatio-temporal approach for global validation and analysis of MODIS aerosol products, *Geophys. Res. Lett.*, *29*(12), 8006, doi:10.1029/2001GL013206.
- Ichoku, C., L. A. Remer, Y. J. Kaufman, R. Levy, D. A. Chu, D. Tanré, and B. N. Holben (2003), MODIS observation of aerosols and estimation of aerosol radiative forcing over southern Africa during SAFARI 2000, *J. Geophys. Res.*, *108*(D13), 8499, doi:10.1029/2002JD002366.
- Ichoku, C., L. A. Remer, and T. F. Eck (2005), Quantitative evaluation and inter-comparison of morning and afternoon MODIS aerosol measurements from Terra and Aqua, *J. Geophys. Res.*, *110*, D10S03, doi:10.1029/2004JD004987.
- Jethva, H., S. K. Satheesh, and J. Srinivasan (2007), Assessment of second-generation MODIS aerosol retrieval (Collection 005) at Kanpur, India, *Geophys. Res. Lett.*, *34*, L19802, doi:10.1029/2007GL029647.
- Kaufman, Y. J., and C. Sendra (1988), Algorithm for atmospheric corrections of visible and near IR satellite imagery, *Int. J. Remote Sens.*, *9*, 1357–1381, doi:10.1080/01431168808954942.
- Kaufman, Y. J., D. Tanre, L. Remer, E. Vermote, A. Chu, and B. N. Holben (1997), Operational remote sensing of tropospheric aerosol over land from EOS Moderate Resolution Imaging Spectroradiometer, *J. Geophys. Res.*, *102*, 17,051–17,067, doi:10.1029/96JD03988.
- Kaufman, Y. J., D. Tanre, B. N. Holben, S. Mattoo, L. A. Remer, T. F. Eck, J. Vaughn, and B. Chatenet (2002), Aerosol radiative impact on spectral solar flux at the surface, derived from principal-plane sky measurements, *J. Atmos. Sci.*, *59*, 635–646, doi:10.1175/1520-0469(2002)059<0635:AROSS>2.0.CO;2.
- Kaufman, Y. J., O. Boucher, D. Tanre, M. Chin, L. A. Remer, and T. Takemura (2005), Aerosol anthropogenic component estimated from satellite data, *Geophys. Res. Lett.*, *32*, L17804, doi:10.1029/2005GL023125.
- Kleidman, R. G., N. T. O'Neill, L. A. Remer, Y. J. Kaufman, T. F. Eck, D. Tanré, and B. N. Holben (2005), Comparison of Moderate Resolution Imaging Spectroradiometer (MODIS) and aerosol robotic network (AERONET) remote-sensing retrievals of aerosol fine mode fraction over ocean, *J. Geophys. Res.*, *110*, D22205, doi:10.1029/2005JD005760.
- Koren, I., L. A. Remer, Y. J. Kaufman, Y. Rudich, and J. V. Martins (2007), On the twilight zone between clouds and aerosols, *Geophys. Res. Lett.*, *34*, L08805, doi:10.1029/2007GL029253.
- Levy, R. C., L. A. Remer, D. Tanré, Y. J. Kaufman, C. Ichoku, B. N. Holben, J. M. Livingston, P. B. Russell, and H. Maring (2003), Evaluation of the Moderate-Resolution Imaging Spectroradiometer (MODIS) retrievals of dust aerosol over the ocean during PRIDE, *J. Geophys. Res.*, *108*(D19), 8594, doi:10.1029/2002JD002460.
- Levy, R. C., L. A. Remer, J. V. Martins, Y. J. Kaufman, A. Plana-Fattori, J. Redemann, P. B. Russell, and B. Wenny (2005), Evaluation of the MODIS aerosol retrievals over ocean and land during CLAMS, *J. Atmos. Sci.*, *62*, 974–992, doi:10.1175/JAS3391.1.
- Levy, R. C., L. A. Remer, and O. Dubovik (2007a), Global aerosol optical properties and application to MODIS aerosol retrieval over land, *J. Geophys. Res.*, *112*, D13210, doi:10.1029/2006JD007815.
- Levy, R. C., L. Remer, S. Mattoo, E. Vermote, and Y. J. Kaufman (2007b), Second-generation algorithm for retrieving aerosol properties over land from MODIS spectral reflectance, *J. Geophys. Res.*, *112*, D13211, doi:10.1029/2006JD007811.
- Li, R.-R., Y. J. Kaufman, B.-C. Gao, and C. O. Davis (2003), Remote sensing of suspended sediments and shallow coastal waters, *IEEE Trans. Geosci. Remote Sens.*, *41*, 559–566.
- Liu, L., A. A. Lacis, B. E. Carlson, M. I. Mishchenko, and B. Cairns (2006), Assessing Goddard Institute for Space Studies ModelE aerosol climatology using satellite and ground-based measurements: A comparison study, *J. Geophys. Res.*, *111*, D20212, doi:10.1029/2006JD007334.
- Livingston, J. M., et al. (2003), Airborne Sun photometer measurements of aerosol optical depth and columnar water vapor during the Puerto Rico Dust Experiment and comparison with land, aircraft, and satellite measurements, *J. Geophys. Res.*, *108*(D19), 8588, doi:10.1029/2002JD002520.
- Martins, J. V., D. Tanré, L. Remer, Y. Kaufman, S. Mattoo, and R. Levy (2002), MODIS Cloud screening for remote sensing of aerosols over oceans using spatial variability, *Geophys. Res. Lett.*, *29*(12), 8009, doi:10.1029/2001GL013252.
- Mishchenko, M. I., I. V. Geogdzhayev, B. Cairns, B. E. Carlson, J. Chowdhary, A. A. Lacis, L. Liu, W. B. Rossow, and L. D. Travis (2007), Past, present, and future of global aerosol climatologies derived from satellite observations: A perspective, *J. Quant. Spectrosc. Radiat. Transfer*, *106*, 325–347, doi:10.1016/j.jqsrt.2007.01.007.
- O'Neill, N. T., T. F. Eck, A. Smirnov, B. N. Holben, and S. Thulasiraman (2003), Spectral discrimination of coarse and fine mode optical depth, *J. Geophys. Res.*, *108*(D17), 4559, doi:10.1029/2002JD002975.
- Redemann, J., B. Schmid, J. A. Eilers, R. Kahn, R. C. Levy, P. B. Russell, J. M. Livingston, P. V. Hobbs, W. L. Smith, and B. N. Holben (2005), Suborbital measurements of spectral aerosol optical depth and its variability at subsatellite grid scales in support of CLAMS 2001, *J. Atmos. Sci.*, *62*(4), 993–1007, doi:10.1175/JAS3387.1.
- Redemann, J., Q. Zhang, B. Schmid, P. B. Russell, J. M. Livingston, H. Jonsson, and L. A. Remer (2006), Assessment of MODIS-derived visible and near-IR aerosol optical properties and their spatial variability in the presence of mineral dust, *Geophys. Res. Lett.*, *33*, L18814, doi:10.1029/2006GL026626.
- Remer, L. A., and Y. J. Kaufman (2006), Aerosol direct radiative effect at the top of the atmosphere over cloud free ocean derived from four years of MODIS data, *Atmos. Chem. Phys.*, *6*, 237–253.
- Remer, L. A., et al. (2002), Validation of MODIS aerosol retrieval over ocean, *Geophys. Res. Lett.*, *29*(12), 8008, doi:10.1029/2001GL013204.
- Remer, L. A., et al. (2005), The MODIS aerosol algorithm, products and validation, *J. Atmos. Sci.*, *62*, 947–973, doi:10.1175/JAS3385.1.
- Remer, L. A., D. Tanré, Y. J. Kaufman, R. C. Levy, and S. Mattoo (2006), Algorithm for remote sensing of tropospheric aerosol from MODIS: Collection 005, Algorithm Theoretical Basis Document, NASA Goddard

- Space Flight Cent., Greenbelt, Md. (Available at http://modis-atmos.gsfc.nasa.gov/reference_atbd.php).
- Russell, P. B., et al. (2007), Multi-grid-cell validation of satellite aerosol property retrievals in INTEX/ITCT/ICARTT 2004, *J. Geophys. Res.*, *112*, D12S09, doi:10.1029/2006JD007606.
- Smirnov, A., B. N. Holben, T. F. Eck, O. Dubovik, and I. Slutsker (2000), Cloud screening and quality control algorithms for the AERONET database, *Remote Sens. Environ.*, *73*, 337–349, doi:10.1016/S0034-4257(00)00109-7.
- Smirnov, A., B. N. Holben, Y. J. Kaufman, O. Dubovik, T. F. Eck, I. Slutsker, C. Pietras, and R. Halthore (2002), Optical properties of atmospheric aerosol in maritime environments, *J. Atmos. Sci.*, *59*, 501–523, doi:10.1175/1520-0469(2002)059<0501:OPOAAI>2.0.CO;2.
- Tanré, D., M. Herman, and Y. Kaufman (1996), Information on the aerosol size distribution contained in the solar reflected spectral radiances, *J. Geophys. Res.*, *101*, 19,043–19,060, doi:10.1029/96JD00333.
- Tanré, D., Y. J. Kaufman, M. Herman, and S. Mattoo (1997), Remote sensing of aerosol properties over oceans using the MODIS/EOS spectral radiances, *J. Geophys. Res.*, *102*, 16,971–16,988, doi:10.1029/96JD03437.
- Tanré, D., L. A. Remer, Y. J. Kaufman, S. Mattoo, P. V. Hobbs, J. M. Livingston, P. B. Russell, and A. Smirnov (1999), Retrieval of aerosol optical thickness and size distribution over ocean from the MODIS Airborne Simulator during TARFOX, *J. Geophys. Res.*, *104*, 2261–2278, doi:10.1029/1998JD200077.
- Torres, O., P. K. Bhartia, J. R. Herman, A. Sinyuk, P. Ginoux, and B. Holben (2002), A long-term record of aerosol optical depth from TOMS observations and comparison to AERONET measurements, *J. Atmos. Sci.*, *59*, 398–413, doi:10.1175/1520-0469(2002)059<0398:ALTROA>2.0.CO;2.
- Wen, G., A. Marshak, and R. F. Cahalan (2006), Impact of 3D clouds on clear sky reflectance and aerosol retrieval in a biomass burning region of Brazil, *Geosci. Remote Sens. Lett.*, *3*, 169–172, doi:10.1109/LGRS.2005.861386.
- Wen, G., A. Marshak, R. F. Cahalan, L. A. Remer, and R. G. Kleidman (2007), 3D aerosol-cloud radiative interaction observed in collocated MODIS and ASTER images of cumulus cloud fields, *J. Geophys. Res.*, *112*, D13204, doi:10.1029/2006JD008267.
- Yu, H., et al. (2006), A review of measurement-based assessments of aerosol direct radiative effect and forcing, *Atmos. Chem. Phys.*, *6*, 613–666.
- Zhang, J., J. S. Reid, and B. N. Holben (2005), An analysis of potential cloud artifacts in MODIS over ocean aerosol thickness products, *Geophys. Res. Lett.*, *32*, L15803, doi:10.1029/2005GL023254.

B. N. Holben, Laboratory for Terrestrial Physics, NASA Goddard Space Flight Center, Greenbelt, MD 20771, USA.

C. Ichoku, R. G. Kleidman, R. C. Levy, J. V. Martins, S. Mattoo, L. A. Remer, and H. Yu, Laboratory for Atmospheres, Code 613.2, NASA Goddard Space Flight Center, Greenbelt, MD 20771, USA. (lorraine.a.remer@nasa.gov)

I. Koren, Weizmann Institute, Rehovot 76100, Israel.

D. Tanré, Laboratoire d'Optique Atmosphérique, F-59655 Villeneuve d'Ascq, France.